Hasan, MSU, Akhtar, N, Rai, AK, Khan, MA, Alfaisal, FM, Alharbi, RS and Hashim, KS

Climatic teleconnection of the future trend of meteorological, GRACE-DSI, and vegetation-conditioned-based drought analysis in the Ganga Basin

Water Supply

Water Supply Vol 24 No 8, 2641 doi: 10.2166/ws.2024.173

Climatic teleconnection of the future trend of meteorological, GRACE-DSI, and vegetation-conditioned-based drought analysis in the Ganga Basin

Mohd Sayeed Ul Hasan[a,b], Nadeem Akhtar[b], Abhishek Kumar Rai[a], Mohd Amir Khan[c,*], Faisal M. Alfaisal[d], Raied Saad Alharbi[d] and Khalid S. Hashim[e]

[a] Centre for Oceans, Rivers, Atmosphere and Land Sciences, Indian Institute of Technology Kharagpur, Kharagpur, West Bengal 721302, India
[b] Department of Civil Engineering, Aliah University, New Town, Kolkata 7000160, India
[c] Department of Civil Engineering, Galgotias College of Engineering, Knowledge Park I, Greater Noida, Uttar Pradesh 201310, India
[d] Department of Civil Engineering, College of Engineering, King Saud University, Riyadh 11421, Saudi Arabia
[e] School of Civil Engineering and Built Environment, Liverpool John Moores University, Liverpool L3 3AF, UK
*Corresponding author. E-mail: amir.khan@galgotiacollege.edu

ABSTRACT

This study assesses drought in the Ganga River Basin using standard precipitation index (SPI), Gravity Recovery and Climate Experiment Drought Severity Index (GRACE-DSI), and vegetation condition index (VCI) via geographic information system (GIS) and non-parametric tests. Future SPI trends show increasing drought severity from 1986 to 2020. GRACE-DSI analysis (2002–2020) indicates a potential rise in drought conditions. VCI computations reveal vegetation health dynamics. Findings suggest an impending severe drought in the Ganga Basin, necessitating urgent water resource management. Drought causes are linked to precipitation changes and resource over-exploitation in changing climate conditions. The study emphasizes implementing measures like water conservation, sustainable land use, and groundwater recharge strategies to mitigate drought impacts.

Key words: climate change, GIS, GRACE-DSI, SPI, teleconnection, VCI

HIGHLIGHTS

- *Integrated drought assessment*: Using GIS and multi-temporal data, this study evaluates SPI, GRACE-DSI, and VCI in the Ganga Basin.
- *Future drought warning*: SPI trends and negative GRACE-DSI slopes signal rising drought risks, emphasizing proactive water resource management.

1. INTRODUCTION

Globally, the research society has focused extensive concern on climate change and fluctuation. It is undeniable that climate change will have an impact on not just disasters but also water quality, biodiversity, and other ecological processes (Hasan & Rai 2020; Jain & Singh 2020; Hasan *et al.* 2022; Aldrees *et al.* 2023). Hydrology is significantly impacted by climate change, which modifies precipitation patterns and the frequency and severity of droughts (Mehta & Yadav 2021; Mehta *et al.* 2023). These modifications upset the components of the water balance, impacting the distribution, quality, and availability of water. This has an impact on the productivity of water usage and raises dangers associated with water. It is anticipated that evapotranspiration will increase, while total runoff may decrease, causing changes in hydrological regimes (Karam *et al.* 2023; Qiu *et al.* 2023). Furthermore, stream flows are increased by more frequent and intense rainfall events, but snowfall is converted to rainfall by higher temperatures, lowering the amount of water stored in the snowpack. Mitigation methods that are tailored to the unique consequences of climate change on hydrology on a regional level are necessary to address these difficulties (Hassan *et al.* 2023). The availability of groundwater and the flow of that water are influenced by topographical, hydrological, biological, geological, and atmospheric variables (Prasad *et al.* 2020; Akhtar & Rampurawala 2024). Therefore, it is vital to study the sustainability of irrigation water management in an agriculturally intensive region to recognize food safety as well as environmental and socioeconomic growth in the context of climate change. Standardized precipitation index (SPI), Gravity Recovery and Climate Experiment (GRACE), and vegetation condition index (VCI) enable the examination of relationships

between meteoroidal, terrestrial, and vegetation droughts under changing climatic conditions, and their teleconnection. The employing of drought index analysis is beneficial for drought assessment in order to consider strategies for reducing, and adapting to climate change (Mehta & Yadav 2022; Mehta *et al.* 2023). The standardizd precipitation index (SPI), which may be hand-me-down to appraise the water dearth in a variety of time periods, is one of the most used indices for this purpose. However, it only considers variations in precipitation levels as its single variable (Jos *et al.* 2022). It is regarded as a global drought index and is operationally used in many hydrological and meteorological services (Cheval 2016).

By calculating the SPI, it is possible to precisely monitor the emergence and worsening of meteorological drought during times of high variability in precipitation patterns (Kubicz 2018). The SPI is employed in the Das *et al.* (2020) study to track the geographic extent and severity of drought events in the Luni River Basin using the long-term precipitation monthly data of 39 rain gauge sites (1973–2016). Major drought episodes were reported in the following years, according to the annual SPI result: 1981, 1984, 1985, 1988, 1989, 1991, 1993, 1999, 2000, 2004, 2005, and 2008. Another study was conducted by Meshram *et al.* (2018), to analyze the Tonnes River Basin's droughts from 1969 to 2008. Drought is detected across the study region using precipitation data collected at four-gauge sites. The 3-month SPI is used to calculate the occurrence of drought. According to their findings, the Allahabad, Rewa, and Satna stations experienced severe drought during the years 1973 and 1979. Recent Multi-Criteria Decision-Making Tool (MCDM) used for drought assessment, flood, ecology, irrigation suitability, and groundwater quality analysis (Rehman *et al.* 2021, 2022; Alharbi *et al.* 2022; Hasan & Rai 2023; Molla *et al.* 2023). The total amount of rainfall between June and November is the main factor influencing the drought pattern in the Tonnes River Basin. In Kalura's (2021) study, the SPI-12 time series was developed using the mean annual rainfall across the basin over 69 years. It was discovered that the Tons basin experienced drought 21 times in total or once every three years. The GRACE-DSI and other modern indices are examined throughout four significant Indian river basins – the Ganga, Krishna, Godavari, and Mahanadi – in order to assess their applicability. Furthermore, it is clear that there have been at least two drought episodes in virtually all of the river basins, with intensities fluctuating from D1 (moderate drought) to D4 (severe drought) (Sinha *et al.* 2019). Rawat *et al.* (2022) studied the GAREC-DSI and CCDI (Climate Change Data Integration), and resulted that when compared to CCDI, GRACE DSI displays strong declining tendencies over the majority of the Indian sub-basins, showing that terrestrial water storage (TWS) depletion is the primary cause of most drought episodes. Satishkumar *et al.* (2020) used combined drought indices, including GRACE-DSI, during 2002–2016 over the Godavari, Krishna, Pennar, and Cauvery river basins, utilizing the Pearson correlation coefficient (*r*). Kamble *et al.* (2021) used Normalized Difference Vegetation Index (NDVI)-based vegetation condition index (VCI) from 2000 to 2015 was used to track agricultural dryness over Allahabad, Kanpur, and Lucknow districts. Another study Quiring & Ganesh (2010), analyzed data from Texas regions to analyze the linkage between the satellite-based VCI and several commonly used meteorological drought indicators during the course of 18 rising periods (March–August, 1982–1999). The temporal and geographical differences in drought were examined in a study conducted in China using VCI data collected from 1982 to 2010 and the result depicts that the VCI improved in the majority of agricultural regions, showing that the occurrence of droughts reduced over time (Qian *et al.* 2016). The southern region saw a more pronounced decline in drought frequency than the northern region. Recent studies in the Ganga Basin show that there is an alarming rate of groundwater over-exploitation over the past two decades leads to the formation of dark zones responsible for the groundwater drought in the Ganga Basin (Hasan *et al.* 2024). Hence, this research serves as a basis for informed decision-making and policy formulation to address the challenges posed by drought in the Ganga River Basin and similar water-stressed regions worldwide. The Ganga Basin is the largest river basin in India, and as such, it is significant because of its diverse geographic extent spanning multiple states, its large population and reliance on irrigation, its vulnerability to climate change, and the complexity of groundwater dynamics. It also provides a comprehensive platform for research on hydrology, climate, agriculture, and human–environment interactions (Kumar 2017; Akhtar 2023) These factors led us to choose the Ganga Basin for our study. This study investigates the relationship between meteorological variables and drought indices in the Ganga Basin, projecting future trends in drought severity. It aims to identify vulnerable regions and guide targeted interventions for adaptation.

2. STUDY AREA

The river Ganga rises in the Gangotri Glacier in Gaumukh and flows through the Uttarkashi district of Uttarakhand, India, with geographic extents of 21°32′ to 31°28′ North Latitude and 73°24′ to 89°5′ East Longitude, and a mean elevation of ~386.12 m above the average sea level is the only the focus of the study (Figure 1). The Ganga River Basin is the greatest

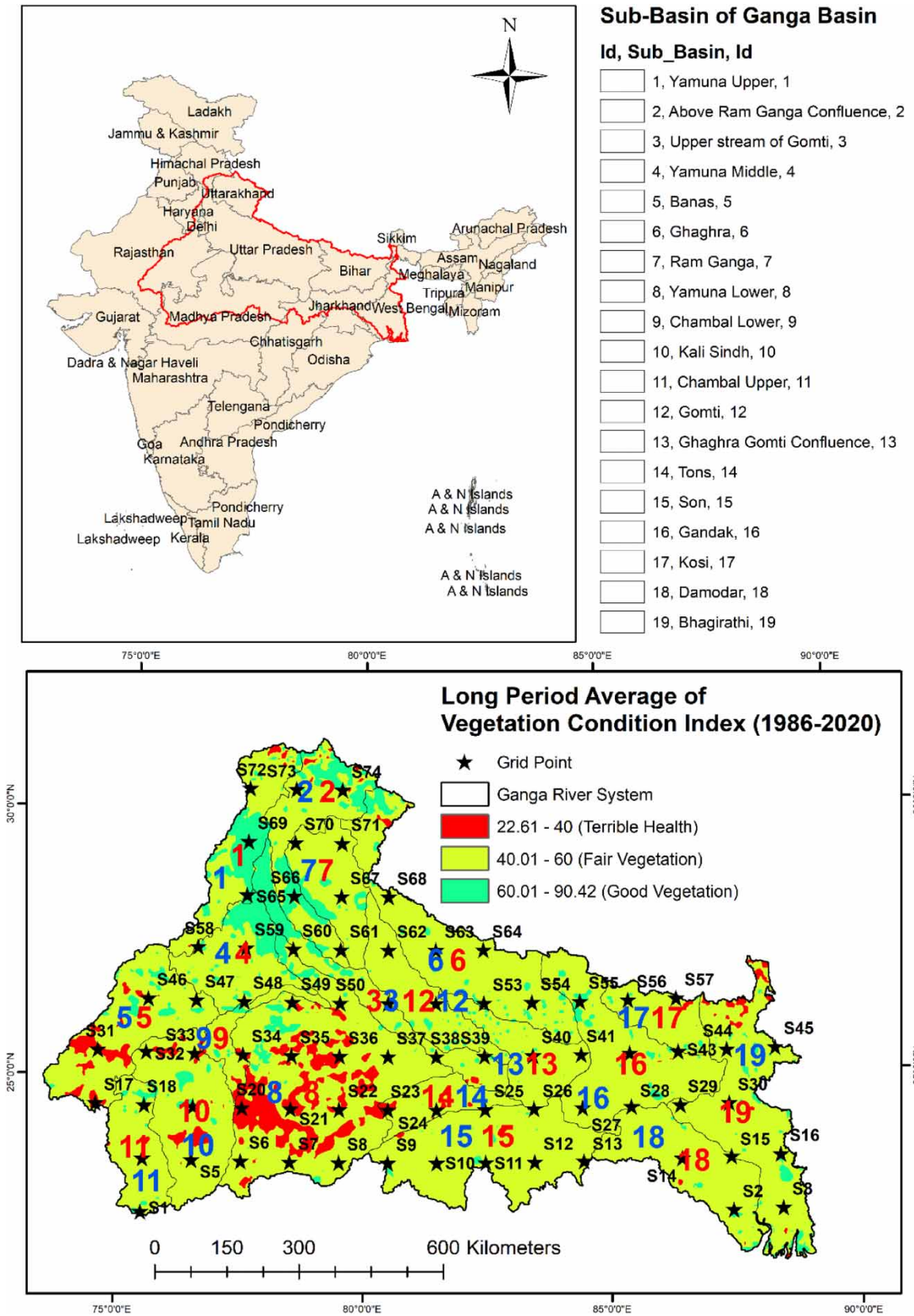

Figure 1 | Study area of the Ganga and sub-basin with grid points (S1–S74) and mean vegetation-conditioned index.

river basin in India and the 4th largest river basin globally (Jain & Singh 2020). The states of, Uttar Pradesh, Uttarakhand, Jharkhand, Bihar, Rajasthan, West Bengal, Punjab, Haryana, Madhya Pradesh, Himachal Pradesh, and Delhi are located in the Ganga Basin of India. Studies using regional climate models in the Ganges basin foresee a rise of 1°–4° in the average yearly temperature from 2010 until 2050 (Moors *et al.* 2011). The Ganga Basin is one of the most irrigated places in the world, with groundwater irrigation used in around 57% of irrigated lands. 8% of the world's population and 0.6% of the world's total land area are in the Ganga basin. In addition, the basin has 10.3% of the world's irrigated land (Siebert *et al.* 2015; Dangar & Mishra 2021).

3. DATA AND METHODOLOGY

The work focuses on the different drought indices based on which different datasets were procured from the different agencies to carry out the work, which is elaborated in detail within the sub-section. This study utilizes three types of data to calculate different drought indices. First, precipitation-gridded data spanning from 1986 to 2020 provides information on precipitation distribution, obtained from India Meteorological Department (IMD)-gridded data with a spatial resolution of 0.25° × 0.25° (Pai *et al.* 2014). Second, recent GRACE monthly mass grids (RL06) from 2002 to 2020, processed at the Jet Propulsion Laboratory (JPL), with a resolution of 1° × 1°, are employed (Landerer & Swenson 2012). Finally, the VCI is derived by integrating NDVI values from National Oceanic and Atmospheric Administration (NOAA) CDR (Climate Data Record) and AVHRR (Advanced Very High-Resolution Radiometer) satellite data covering the period from 1986 to 2020 having a spatial resolution of 0.05° × 0.05° (Vermote & NOAA CDR 2019, 2022).

3.1. Standard precipitation index

As per the guiding principle of the World Meteorological Organization, the sole input parameter needed for the SPI's extensive drought forecasting index is precipitation. It has been frequently used to represent meteorologically thirsty spells and is seen to be a database of the result to represent meteorological droughts. Since it is simple to use, geographically stable with the analysis, and predictive thereby it may be utilized throughout hazard planning and process modeling, and is customizable to the time periods of the recipient's concern, it continues to be a popular option among researchers in drought studies (Meshram *et al.* 2018). McKee *et al.* (1993) introduced the SPI, and a drought scenario happens when the SPI values are consistently low and sink to a level of 1 or below. However, the dry spell terminates once the SPI numbers are greater than 0. Consequently, the length and intensity of each drought period may be used to characterize it. It enables us to determine if a drought will occur at a certain timeline of interest for any precipitation station with historical data. When using long-term precipitation data for the relevant time period, the SPI is determined for any place. The long-term data are equipped having a gamma probability distribution function, which is converted into an ordinary dispersal to a generate zero median SPI for the specific place and time period. The negative and high SPI values, respectively, represent below-average and above-average precipitation. Precipitation below the average suggests dryness, whereas precipitation over the median suggests wetness occurrences (Tefera & Bello 2019; Ahmad *et al.* 2022; Mohammed *et al.* 2022).

The SPI is referred to as the degree of standard deviations that occur when the reported precipitation differs from the continuing average for an evenly spaced unpredictable component after the precipitation is translated into normalized numerical values. SPI is less complicated to use than other drought indicators since it just needs a single input feature for the collection of long-term precipitation (Tirivarombo *et al.* 2018). The SPI is ideal for both agricultural and hydrological purposes because of its temporal flexibility. Any zone's SPI computation depends on the continuing precipitation history for the chosen span of time. During the SPI, if it is continually negative and reaches a power level of −1.0 or below, a drought event happens. In the case of a positive SPI, the event is over. Therefore, the beginning, the end, and the severity of each month of a drought period determine its long-term existence (Meshram *et al.* 2018). The long-term daily precipitation data were procured from IMD for the period of 36 years (1986–2020) (Pai *et al.* 2014). A drought in the weather can have several negative repercussions, and as SPI may be computed crosswise various precipitation growth periods there are numerous SPI gauges that can be used to estimate these effects. In this work, we computed SPI-3, SPI-6, SPI-9, and SPI-12. SPI-3 evaluates short-term drought conditions, which is vital for agricultural planning (Hadri *et al.* 2021); SPI-6 identifies extended dry periods impacting water availability, soil moisture, and vegetation (Sazib *et al.* 2018); SPI-9 aids in comprehending persistent droughts affecting groundwater levels, reservoirs, and ecosystems (Liu *et al.* 2019); SPI-12 is essential for water resource management, hydrological planning, and gauging drought's overall impact on ecosystems and communities (Rezaiy & Shabri 2023).

When calculating the SPI using Equations (1)–(5), a station's total precipitation frequency distribution is estimated with a gamma probability distribution function (Shah *et al.* 2015). The frequency or probability exponential distribution serves as the definition of the gamma distribution.

$$g(x) = \frac{1}{\beta^{\alpha}\Gamma(\alpha)} x^{\alpha-1} e^{-x/\emptyset} \tag{1}$$

when the gamma probability distribution function's alpha (α) > 0 shape factor and beta (β) > 0 scale parameter are estimated over timeframes of 3 months at each station (Meshram *et al.* 2018).

$$\Gamma(\alpha) = \int_0^{\infty} y^{\alpha-1} e^{-y}$$

where $\Gamma(\alpha)$ represents the gamma component (Shah *et al.* 2015).

A frequency analysis of the total quantity of precipitation at a station is used to compute the SPI by adapting a gamma density function of probabilities to it. To estimate α and β as best as possible, the maximum likelihood solutions are applied:

$$\alpha = \frac{1}{4A}\left(1 + \sqrt{1 + \frac{4A}{3}}\right)$$

$$\beta = \frac{\bar{x}}{\mu}$$

$$A = In(\bar{x}) - \frac{\sum In(x)}{n}$$

where n is the number of rainfall stations. The accumulated likelihood is given by:

$$G(x) = \int_0^x g(x)dx = \frac{1}{\beta^{\alpha}\Gamma(\alpha)} \int_0^x x^{\alpha-1} e^{-x/} \phi dx \tag{2}$$

Letting $t = X/\beta$, the formula becomes the gamma function that is not complete.

$$G(x) = \frac{1}{\Gamma\alpha} \int_0^x t^{a-1} e^{-t}\, dt = \frac{1}{\Gamma(\alpha)} \sum_{t=0}^{t} t^{\alpha-1} e^{-b}$$

The accumulated likelihood is as follows when $x = 0$ and the gamma function cannot be defined:

$$C(x) = q + (1 - q)G(x) \tag{3}$$

where q is the likelihood of a zero, and $C(x)$ is an accumulated likelihood.

Using the approximate conversion method, the accumulated possibility is then converted to the normalized arbitrary variable Z, which is the rate of the SPI: (Meshram *et al.* 2018)

$$Z = \text{SPI} = -\left(t - \frac{c_0 + c_1 t + c_2 t^2}{1 + d_1 t + d_2 t^2 + d_3 t^3}\right) \tag{4}$$

for $0.5 \geq C(x) > 0$

$$Z = \text{SPI} = +\left(t - \frac{c_0 + c_1 t + c_2 t^2}{1 + d_1 t + d_2 t^2 + d_3 t^3}\right) \tag{5}$$

for $1.0 \geq C(x) > 0.5$

$$t = \sqrt{\ln\left(\frac{1}{(C(x))^2}\right)}$$

for $0.5 \geq C(x) > 0$

$$t = \sqrt{\ln\left(\frac{1}{1.0 - (C(x))^2}\right)}$$

for $1.0 \geq C(x) > 0.5$

$C_0 = 2.515517,\ C_1 = 0.802853,\ C_2 = 0.010328,$

$d_1 = 1.432788,\ d_2 = 0.189269,\ d_3 = 0.001308$

An SPI value of 1 and above indicates that a wet event has occurred. $Z > 2.0$ values designate extremely heavy rainfall over the designated timeframe. A SPI result between $1 > Z > -1$ indicates a rainfall event that is roughly typical. Furthermore, drought occurrences are directed by a Z-score of -1 or less. The presence of a severe drought is indicated when the Z-score is less than -1.5 (Table 1) (Meshram *et al.* 2018).

3.2. Gravity Recovery and Climate Experiment Drought Severity Index (GRACE-DSI)

National Aeronautics and Space Administration (NASA) and Deutsches Zentrum für Luft- und Raumfahrt (German Aerospace Center) collaboratively developed the GRACE mission in March 2002 (Cheng & Tapley 2004; Rodell *et al.* 2004; Jacob *et al.* 2012; Landerer & Swenson 2012; Hasan *et al.* 2023). Two satellites were launched as part of the GRACE project, one after the other in a near-polar orbit ~500 km above the Earth's surface, separated by ~220 km (Vishwakarma 2020). The mission's primary goal consists of precisely gauging the Earth's gravity influence each month (Mukherjee & Ramachandran 2018). In this study, the analysis is based on the most recent GRACE monthly mass grids (RL06) processed at the JPL having $1° \times 1°$ resolution from 2002 to 2020. Another advantage of RL06 is that, over coastlines, the signal leakage errors are decreased by the coastal resolution improvement filter to improve the data accuracy of GRACE Terrestrial Water Storage Anomaly (TWSAs) (Wiese *et al.* 2016). Monthly mean TWSA irregularities, which are like rainwater collection anomalies and water height, are used to express the estimated mass variances of GRACE acquired by monitoring the temporal fluctuation in gravity. A water mass balance technique is used to calculate variations in available water storage (combined conservation of groundwater and surface reservoir variations) in any basin. The various TWSA components consisting of soil moisture (SM), snow water equivalent, surface water (SW), and ground water are all included in the TWS anomaly

Table 1 | Categorization of SPIs depending on their range values (McKee *et al.* 1993)

SPI range	Category
+2 or more	Extremely wet
1.55–1.99	Very wet
1.00–1.49	Moderately wet
−0.99 to 0.99	Near-normal
−1.00 to −1.49	Moderately dry
−1.5 to −1.99	Severely dry
−2 to less	Extremely dry

measurement (Singh *et al.* 2018):

$$TWS_t = SM_t + SWE_t + SW_t + GW_t$$

where the function of time is indicated by the subscript t. Successful drought mitigation measures may be transferred to different places with the use of drought monitoring and research based on standardized drought indices. Since it is a standardized drought measure that takes into consideration the geographical fluctuation in TWS that directly influences the characterization of drought (Liu *et al.* 2020). The standardized aberrations of GRACE TWS are what the GRACE-DSI is described as (Zhao *et al.* 2017; Gerdener *et al.* 2020) using Equation (6):

$$GRACE - DSI_{i,j} = \frac{TWS_{i,j} - \overline{TWS_j}}{\sigma_j} \tag{6}$$

where i is the years that range from 2002 to 2020 and j is a season that ranges from premonsoon, summer, monsoon, postmonsoon to annual, $\overline{TWS_j}$ and σ_j are, respectively, the average and standard deviation of $TWSA$ differences in seasonal j (Table 2).

3.3. Vegetation condition index

By combining the NDVI values from NOAA CDR and AVHRR satellite data (Vermote 2019, 2022), the VCI was computed as it can differentiate between short-term climatic cues and long-term biological signals. VCI acts as a more accurate indication of SM sensitivity than NDVI. VCI compares the NDVI data for a certain time to the maximum (max) and lowest (min) data values of the NDVI values pertaining to the whole period under consideration. VCI is a percentage (%) that indicates the most and least values of the measured data over the course of the previous year and is calculated as below (Aksel 2021) using the following equation:

$$VCI = \frac{NDVI_{curr} - NDVI_{min}}{NDVI_{max} - NDVI_{min}} \times 100 \tag{7}$$

High VCI readings (60–100)% show that the vegetation was in good condition, in contrast to the low VCI values (0–40)% that show that the vegetation is in terrible health. Moreover, moderate values (40–60)% represent the fair vegetation index (from the Drought Management Manual, Govt. of India). The normalization is used to reduce the impact of spatial patterns in NDVI vegetation between various land cover types and climatic conditions and to emphasize comparative shifts in the local NDVI signal over time (Boqer & Science 2009).

Table 2 | The GRACE-DSI is a dimensionless measure for detecting drought and unusually damp conditions (Zhao *et al.* 2017)

Category	Description	GRACE-DSI
W4	Exceptionally wet	2.0 or more
W3	Extremely wet	Between 1.60 and 1.99
W2	Very wet	Between 1.30 and 1.59
W1	Moderately wet	Between 0.80 and 1.29
W0	Slightly wet	Between 0.50 and 0.79
WD	Near-normal	Between 0.49 and −0.49
D0	Abnormally dry	Between −0.50 and −0.79
D1	Moderate drought	Between −0.80 and −1.29
D2	Severe drought	Between −1.30 and −1.59
D3	Extreme drought	Between −1.60 and −1.99
D4	Exception drought	−2.0 or below

3.4. Modified Mann–Kendall test (MMK)

The Mann–Kendall test was employed to assess climatic changes in different places worldwide. The following procedure was used to calculate the outline of the statistical test for the MMK test (Hamed & Rao 1998; Jena *et al.* 2021):

$$S_0 = \sum_{k=1}^{n-1} \sum_{k+1}^{n} \text{sign}(x_j - x_k); j > k \tag{8}$$

where n is the number of observations, x is the dynamic time warping (DTW) trend analysis, and j and k, correspondingly, between 2 and n and 1 to $n-1$ (Gocic & Trajkovic 2013). The readings are likely to be greater (relatively small) than earlier reports, according to a positive (negative) value for S_0. When the results are positively (negatively) autocorrelated, the deviation of S_0 is drastically underestimated (overestimated). For a mMK test, the modified variable is computed as follows (Ahmadi *et al.* 2018):

$$V^*(S_0) = \text{var}(S_0) \times \frac{n}{n_S^*} = \frac{n(n-1)(2n+5)}{18} \times \frac{n}{n_S^*} \tag{9}$$

where $V(S_0)$ is the modified variances and n/n_S is the correction factor specified by:

$$\frac{n}{n_S^*} = 1 + \frac{2}{n(n-1)(n-2)} \times \sum_{i=1}^{n-1} (n-1)(n-i-1)(n-i-2)\rho_S(i)$$

when n_S is regarded as an appropriate number of samples required to account for the autocorrelation in the rank, i ranges from 1 to $n-1$, and ρ_S is the autocorrelation function of the ranks of the remarks. When there are more than 10 samples, the standard normal variable Z is calculated as:

$$Z = \begin{cases} \dfrac{S-1}{\sqrt{V^*(S_0)}} & if\ S_0 > 0 \\ 0 & if\ S_0 = 0 \\ \dfrac{S+1}{\sqrt{V^*(S_0)}} & if\ S_0 < 0 \end{cases}$$

A dropping trend for DTW is made known by positive Z values, and a rising drift is indicated by negative Z values. The assumption or hypothesis (H_0) is validated if $|Z_S| < Z_{0.05/2}$ for a specific statistical significance; otherwise, it is discarded. Figure 2 presents the thematic flowchart of the adopted methodology.

4. MODELING RESULTS

4.1. Standard precipitation index (SPI)

4.1.1. Descriptive analysis of SPI-3

The SPI-3, which is connected to 3 months' average rainfall accumulation, is a drought indicator used to identify the direct effects of drought. As per our analysis of the 3-month SPI, a total of 418 occurrences were recorded at each of the 74 sites we chose throughout the Ganga River basin over the specified time period (Figure 3). We found that the largest individual drought event recorded during the whole period of the study was near-normal rainfall conditions (i.e., 24,520), while the lowest was extreme drought conditions (i.e., 439) after doing a frequency analysis for full drought events comprising all grid points. In addition, although an extreme drought occurred 13 times at grid S-35 by following grid S-8 (12 times) and S-2, S-20, and S-27 (every 11 times) during the course of the period, it only happened once at grid S-24, S-47, S-53, and S-55. The total number of severe drought events that occurred was 1,050, and we found that the grid with the fewest severe drought events (6 times) was S-3 and S-30, whereas grid S-69 had the most severe drought events (31 times). If we

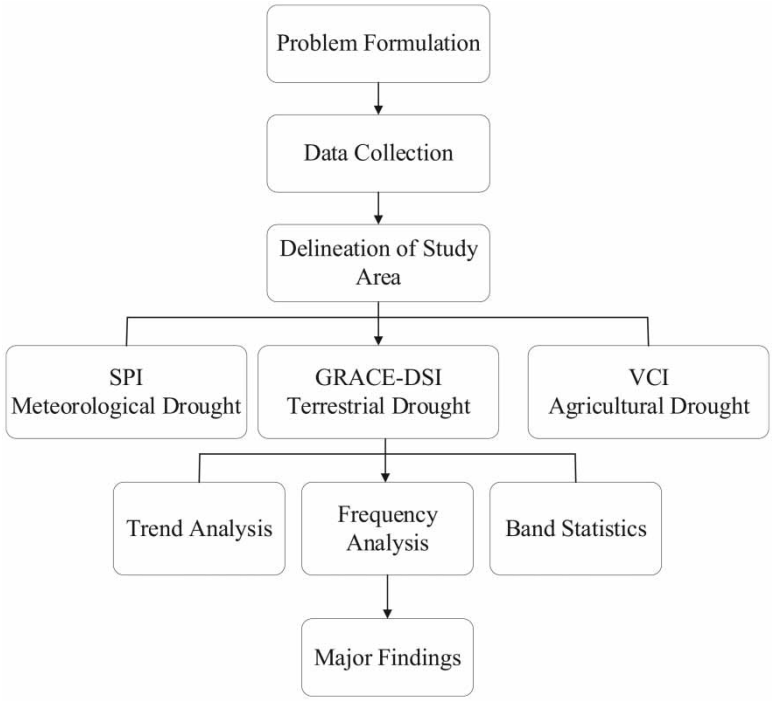

Figure 2 | Adopted methodology.

talk about wet circumstances, there are a total of 1,359 very wet and 2,839 moderately wet occurrences, as well as 725 extreme wet events in which grid S-29 and S-60 independently recorded the greatest (16 times) and lowest (4 times) extreme wet conditions, respectively. There is not a single case of a moderate drought event recorded in the SPI-3 analysis over the study area.

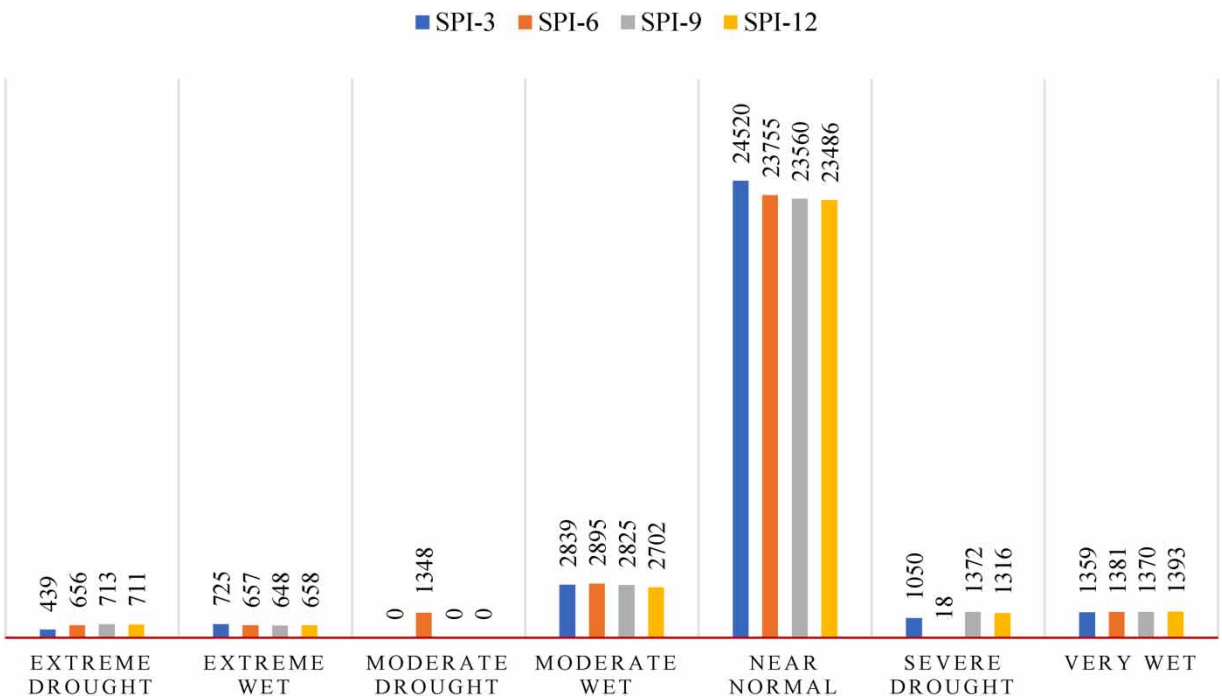

Figure 3 | Frequency analysis of SPI-3, SPI-6, SPI-9, and SPI-12 (*y*-axis – number of events).

The analysis of the 3-month standardized precipitation index (SPI3) reveals diverse trends in precipitation across different regions (Figure 4(a)). Out of the 74 grid points examined, it can be observed that 12 grids have experienced a significant decreasing trend (SDT), as evidenced by a *Z*-Significance value less than −1.96. This implies that there has been a notable reduction in precipitation in those regions over the 3-month period. Conversely, the 31 grid exhibits a non-significant decreasing trend (NSDT), with a *Z*-significance value between 0 and −1.96, suggesting a downward trend in precipitation, although not statistically significant. Similarly, there are 25 grids with a non-significant increasing trend (NSIT), as their *Z*-significance value ranges from 0 to 1.96, indicating a mild upward trend in precipitation. Conversely, five grids have a significant increasing trend (SIT), with a *Z*-significance value greater than 1.96, showing a marked increase in precipitation. Only one grid had no trend, as its *Z*-significance value was 0, implying no significant variation in precipitation. Therefore, the data highlight the considerable variability in SPI3 trends among different regions, with some areas experiencing significant changes in precipitation, while others demonstrate non-significant trends in either direction.

Based on the zonal statistics, the minimum Sen's slope values range from −0.002705 to −0.000112 (Table 3). The sub-basin with the very minimum Sen's slope value is Bhagirathi, with a value of −0.002705. The other sub-basins with relatively low Sen's slope values (below −0.0015) are Yamuna Lower, Ghaghra, Ram Ganga, Gandak, and Kosi. Most of the sub-basins have Sen's slope values between −0.0015 and −0.0005, indicating moderate to low levels of precipitation.

Overall, the analysis suggests that the precipitation levels in most of the sub-basins are within normal ranges, although some sub-basins have experienced lower precipitation levels than others (Figure 4(a)). The very minimum value experienced sub-basin is Bhagirathi. The maximum Sen's slope value was observed at 0.001186 in Yamuna Upper, which is the highest value among all sub-basins. On the other hand, the least maximum value is observed in Bhagirathi, which is 0. Among the sub-basins, some of the other notable maximum Sen's slope values are observed in Ram Ganga (0.001102), Yamuna Middle (0.001014), Banas (0.000796), and Kali Sindh (0.000886). The sub-basins with relatively lower maximum Sen's slope

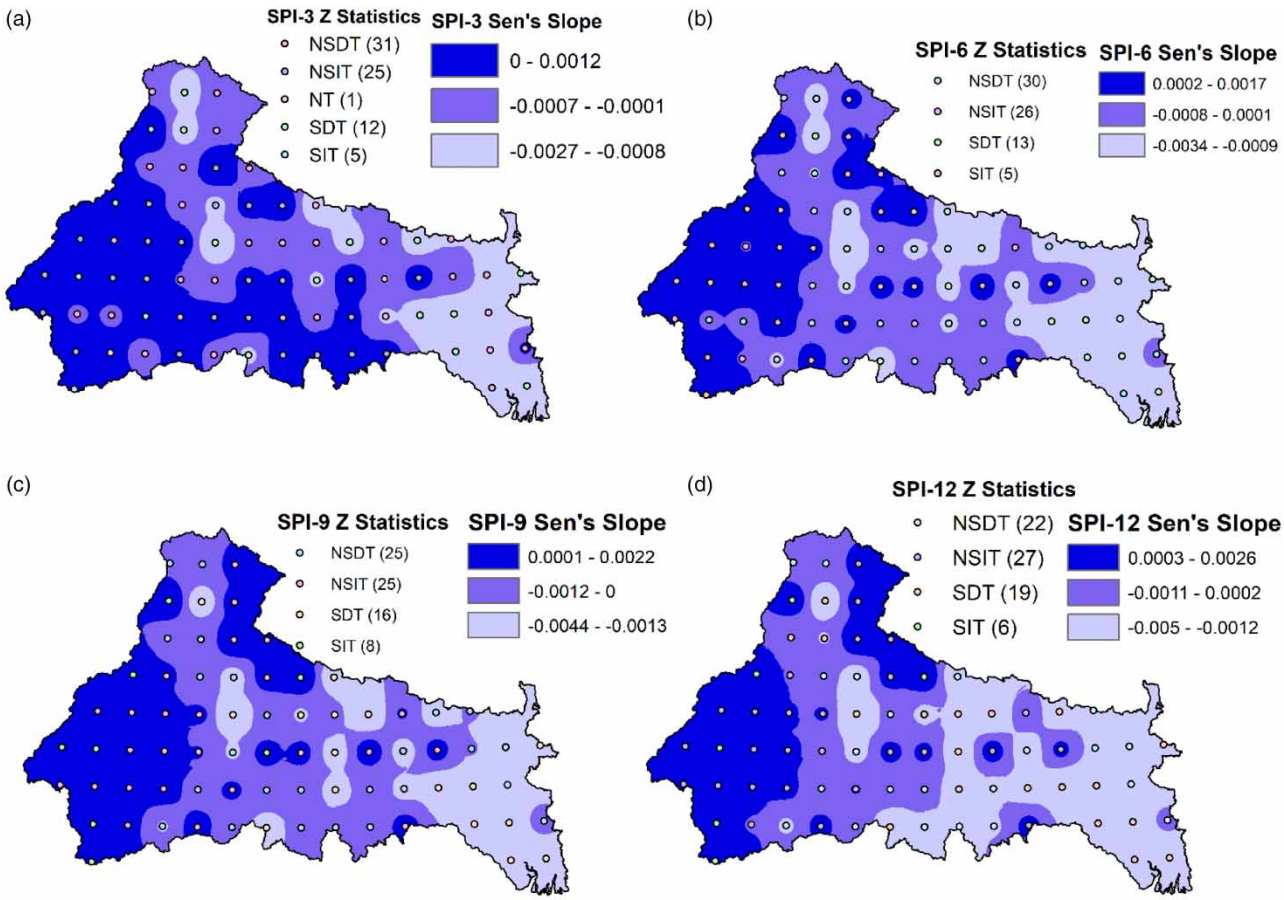

Figure 4 | Future trend of SPI using MMK and Sen's slope.

Table 3 | Band statistics of SPI in the Ganga Basin

Build parameter	SPI-3	SPI-6	SPI-9	SPI-12
Minimum value	−0.003	−0.003	−0.004	−0.005
Maximum value	0.001	0.001	0.002	0.003
Mean value	−0.0003	−0.0003	−0.0005	0.0006
Standard deviation	0.0005	0.0008	0.0011	0.0013

values include Tons (0.000152), Above Ram Ganga Confluence (0.000132), and Kosi (−0.000102). The mean SPI-3 Sen's slope values range from −0.001142 to 0.000377 (Figure 5). The Bhagirathi sub-basin has the lowest mean Sen's slope value of −0.001142, indicating that it has the driest conditions. The Damodar sub-basin has the second-lowest mean Sen's slope value of −0.001054, which suggests that it also has dry conditions. The Yamuna Upper sub-basin has the highest mean Sen's slope value of 0.000023, indicating that it has the wettest conditions. The Chambal Upper and Banas sub-basins also have positive mean Sen's slope values, indicating relatively wet conditions. Most sub-basins (13 out of 19) have negative mean Sen's slope values, indicating that they have dry conditions. The range of mean Sen's slope values is relatively small, with the difference between the wettest and driest sub-basins being less than 0.002.

4.1.2. Descriptive analysis of SPI-6

The 6-month SPI is particularly effective in visualizing precipitation over the course of the seasons and identifying seasonal to medium-term variations in precipitation (Pandey & Rao 2019). Our SPI-6 analysis includes 74 locations with a total of 415 incidents at each grid; the majority of them occur under near-normal circumstances (23,755) while the fewest events occur under severe drought conditions (only 18 times). In addition, the frequency of both extremely dry and extremely wet circumstances is almost equal (656 and 657, respectively). Furthermore, the frequency of extreme drought episodes was lowest at grids S-47, S-6, and S-13 (only 2 times), while it was greater (21 times) at grids S-20 and S-60, and at site S-24, no extreme drought event happened throughout the period. Several grids, including S-4, S-10, S-13, S-15, S-23, S-34, S-50, S-56, S-57, S-64, S-67, and S-69, have only experienced severe drought once; S-27 has encountered it twice; and S-62 has suffered it

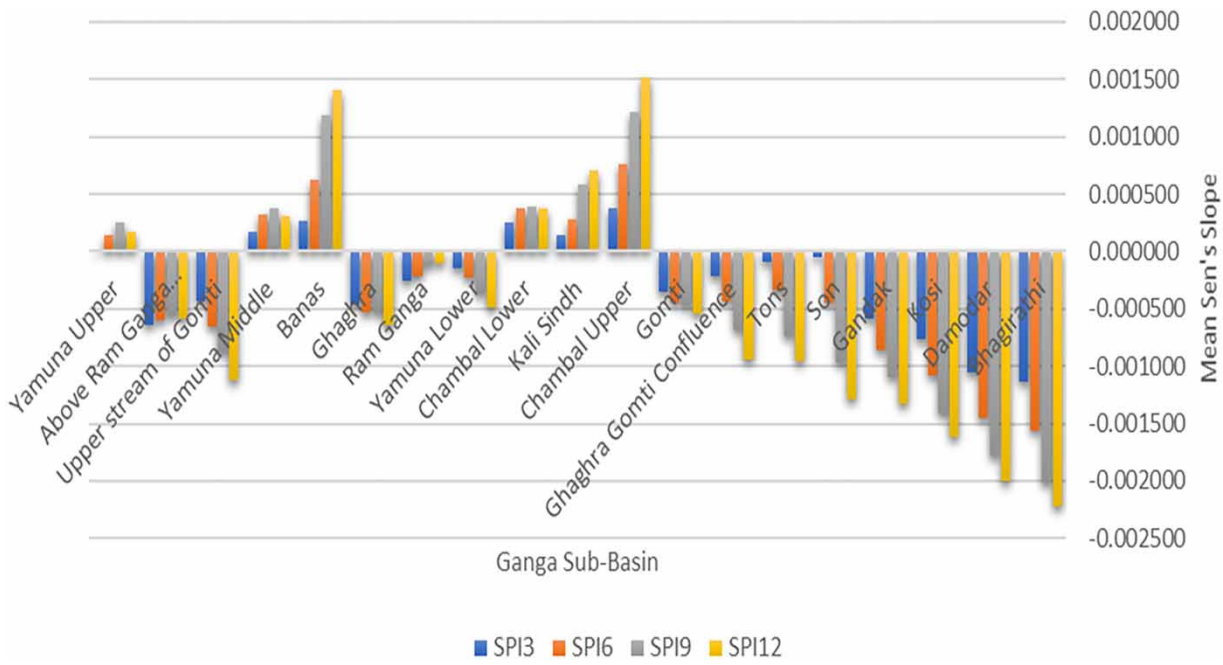

Figure 5 | Zonal statistical mean of sub-basins in the Ganga River system.

three times; the rest of the sites did not experience any severe drought circumstances. Moderate drought occurrences now happen most frequently (30 times) at grid S-13 and least frequently (8 times) at grid S-72. On the other side, conditions that were extremely wet, very wet, and moderately wet were detected 657, 1,381, and 2,895 times, respectively.

The study examined 74 grids to determine trends in SPI6, a measure of drought conditions (Figure 4(b)). Of this grid, 5 (6.76%) exhibited a SIT in SPI6, indicating a worsening of drought conditions over time in those regions. A total of 26 grids (35.14%) showed a non-significant increasing trend, suggesting that there may be some increase in drought conditions, but it is not statistically significant. On the other hand, 30 grids (40.54%) showed a non-significant decreasing trend, implying some improvement in drought conditions, but it is not statistically significant. The remaining 13 grids (17.57%) displayed a significant decreasing trend in SPI6, suggesting that drought conditions are improving over time in those regions. Therefore, it can be concluded that the majority of the grid (65.68%) shows either a non-significant or an SIT in SPI6, indicating that drought conditions are generally getting worse over time in the study region.

The SPI-6 is a measure of drought intensity based on the precipitation data for a period of 6 months. The zonal statistical Sen's slope minimum of all sub-basins except Banas and Bhagirathi have negative values, indicating that these areas have experienced drought conditions over the past 6 months. Yamuna Lower, Chambal Lower, Ram Ganga, and Ghaghra have the lowest minimum Sen slope values, indicating that these areas have experienced the most severe drought conditions. Kali Sindh and Chambal Upper have the least severe drought conditions among the sub-basins with negative values. The highest Sen's slope of SPI-6 value is 0.001739 for the Chambal Upper sub-basin, and the lowest Sen's slope value is −0.000385 for the Kosi sub-basin. The Sen's slope values for most sub-basins are positive, indicating an increasing trend in precipitation over time. The highest positive Sen slope values are observed for the Chambal Upper, Yamuna Middle, Ram Ganga, Ghaghra, and Banas sub-basins. However, two sub-basins, Kosi, and Bhagirathi, show negative Sen's slope values, which indicate a decreasing trend in precipitation over time. With a Sen's slope value of 0.000043, the Tons sub-basin has the lowest slope, indicating a rather steady trend in precipitation. The Sen's slope values for the sub-basins range widely, from −0.000385 to 0.001739, demonstrating that the trends in precipitation in the various sub-basins are not all the same. Only six of the 19 sub-basins (Banas, Chambal Lower, Kali Sindh, and Chambal Upper) have a positive mean SPI-6 score (Figure 5), which denotes a wetter-than-average condition. The SPI-6 value for the remaining 13 sub-basins is negative, which indicates a drier-than-average situation. Bhagirathi is the sub-basin with the lowest mean SPI-6 rating, signifying the worst level of drought. The values range from −0.001559 for Bhagirathi to 0.000760 for Chambal Upper, which shows a substantial difference in the severity of the drought between the sub-basins.

Overall, the analysis reveals that most of the sub-basins are currently experiencing drought conditions, with only a few having above-average precipitation levels.

Overall, the analysis of the standard deviation of Sen's slope values of precipitation data for 19 sub-basins suggests that there is significant variability in precipitation data among the sub-basins. The sub-basins with higher standard deviation values need more attention for better water management practices. The sub-basins with lower standard deviation values can be used as benchmarks for comparison and evaluation of other sub-basins.

4.1.3. Descriptive analysis of SPI-9

The SPI-9 gives information on inter-seasonal precipitation patterns at a time range of medium intervals. Droughts typically take a season or more to emerge (Pandey & Rao 2019). The analysis of the nine-month SPI reveals that we looked at 74 research locations, with 412 incidents at each grid (Figure 3). Near-normal circumstances saw the greatest number of incidents (23,560), while extremely wet conditions saw the least number of events (648). If we were to discuss each category separately, grid S-60 had the most extreme drought incidents (27), whereas grids S-23, S-24, and S-65 experienced the fewest (only 2); additionally, there was no severe drought occurrence at grid S-71. The grids with the highest frequency of severe drought (32 times each) are S-41, S-57, S-68, and S-73, while S-72 has the lowest frequency. However, the study areas as a whole had 648, 1,370, and 2,825 occurrences for the extremely wet, very wet, and moderately wet circumstances, respectively.

Out of the 74 grid points, 8 grids (approximately 11%) show a SIT in SPI9, indicating a consistent increase in precipitation over the 9-month period (Figure 4(c)). This trend could be related to factors such as climate change or natural variability in weather patterns. Around 35% of the grid (26 out of 74) show an NSIT in SPI9. This means that these grids have a slight increase in precipitation over the 9-month period, but the trend is not statistically significant. These trends could be related to natural variability in the weather patterns or local factors such as land-use changes or urbanization. Similar to the previous

instance, a modest drop in precipitation throughout the nine months is shown by 24 out of 74 grids (or roughly 32%), but the trend is not statistically significant. Once more, these developments can be attributed to local variables like urbanization or changes in land use. A substantial declining trend in SPI9 is present in almost 22% of the grid (16 out of 74), showing a steady decline in precipitation over the past 9 months. This pattern may be influenced by variables like climate change or climatic fluctuations. It is crucial to remember that the trends found in SPI9 may have a big impact on the research region. For instance, major trends in precipitation could cause flooding and effects on infrastructure, while significant trends in precipitation could cause drought conditions, water scarcity, and implications on agriculture. The trends in SPI9 should also be taken into account in light of additional variables such as climate change, urbanization, and changes in land use. For instance, increasing urbanization and land-use changes may alter precipitation patterns, while climate change may increase the frequency of extreme weather events like floods and droughts. The majority of sub-basins have negative minimum values, which show a decreasing tendency in precipitation over time as captured by the data (Figure 5). Bhagirathi, which has a minimum value of −0.004407, is the sub-basin with the most negative value, followed by Yamuna Lower, Ram Ganga, and Ghaghra, which have minimum values of −0.004167, −0.003125, and −0.003125, respectively. This shows that the amount of precipitation in these sub-basins has significantly decreased during the research period. On the other hand, several sub-basins, such as Banas, Chambal Upper, and Kali Sindh, show slightly positive or close to zero minimum values, indicating a rather consistent trend in precipitation. The analysis as a whole indicates that most sub-basins in the examined area are seeing a decreasing trend in precipitation, which may have important repercussions for the region's management of water resources and environmental sustainability. With values of 0.002222, Yamuna Middle, 0.002187, and 0.002076, respectively, the Ghaghra sub-basin has the highest maximum Sen's slope value. The highest maximum Sen's slope value is found in the Chambal Upper sub-basin. Precipitation has been increasing in these sub-basins during the past few years, which may be due to climate change or natural variability. However, the maximum Sen's slope values for the Tons, Kosi, and Bhagirathi sub-basins are negative, showing a tendency for precipitation decline. The greatest Sen's slope value for Tons is −0.000051, and the highest values for Bhagirathi and Kosi are −0.000478 and −0.000561, respectively. Less precipitation is experienced in these sub-basins, which may cause drought and a shortage of water. The other sub-basins maximum Sen's slope values range from 0.000714 to 0.001826, which suggests a generally steady trend in precipitation through time. This does not necessarily imply that there has been no change in the amount of precipitation; rather, it simply means that the change has not been sufficiently significant to reveal a definite trend. To maintain sustainable water use and lower the risk of flooding, it is important to monitor and carefully manage the sub-basins with increasing precipitation trends. The effects of water shortage and drought can be reduced by paying attention to the sub-basins with decreasing precipitation trends. According to Figure 5, the zonal statistical mean values range from −0.002022 for the Bhagirathi sub-basin to 0.001219 for the Chambal Upper sub-basin. Examining the results reveals that most sub-basins have negative mean Sen's slope values, which point to a trend in precipitation that is declining with time. The sub-basins Bhagirathi, Damodar, Kosi, Gandak, and Son have the most negative values. This may indicate that these sub-basins are being more severely affected by climate change in terms of precipitation decline. However, several sub-basins such as the Chambal Upper, Kali Sindh, Banas, and Tons sub-basins have positive mean Sen's slope values, which could indicate a long-term tendency of increasing precipitation. This would also suggest that some sub-basins are less severely affected by climate change and might even gain from more precipitation.

4.1.4. Descriptive analysis of SPI-12

In general, 12-month SPI values are related to stream flows, reservoir levels, and even groundwater levels over long time frames (Pandey & Rao 2019). A total of 409 occurrences are recorded at each of the 74 sites that are under analysis. The majority of events (23,486) according to the SPI-12 study results are in close to average weather, whereas the least number of incidents are associated with extremely wet weather (658) (Figure 3). Furthermore, a total of 711 incidents occurred under extreme drought conditions, occurring just once at certain grids (S-21, S-28, S-37, S-43, S-53, S-54, S-55, S-67, and S-71), and 28 times at grid S-8. These conditions never occurred at grids S-12, S-25, and S-29 throughout the entire study period. Moreover, just one instance of a severe drought occurred at grid S-72, whereas the highest 38 instances occurred at grid S-41. On the other hand, there have been 658, 1,393, and 2,702 observations of extremely wet, very wet, and moderately wet incidents, respectively.

The study investigated the trends in SPI12 values across 74 grids in the study region (Figure 4(d)). Of these, 8% or 6 grids exhibit a SIT in SPI12 values, indicating an improvement in drought conditions over these regions. However, due to the absence of information regarding the geographical distribution of this grid, it is not possible to draw any overarching

conclusions about the improvement of drought conditions across the entire study region. However, 36% of the grids, or 27 grids, exhibit NSIT in the SPI-12 values, suggesting a general tendency of increasing precipitation over these areas. Despite not being statistically significant, this tendency may nonetheless be beneficial for a number of industries, like agriculture and water supplies, which rely on rainfall. On the other hand, SPI-12 values of over 30% of the grids, or 22 grids, show an NSDT, which indicates a general pattern of decreasing precipitation over these regions. Agriculture, water supply, and other industries that depend on rain might all suffer from such a decline. 19 out of the 74 grids, or 26%, show a significant decreasing trend (SDT) in SPI-12 values, which indicates a marked deterioration in the drought conditions in these areas. The consequences of this could include crop failures, water shortages, and other negative effects on the environment and society. To reduce the detrimental consequences of drought conditions in many sectors, it is important to address these challenges.

First, the Bhagirathi sub-basin has the lowest minimum Sen's slope value of −0.00503, indicating that it has the most severe drought condition in terms of the SPI_12 analysis (Figure 4(d)). Second, the sub-basins of Yamuna Upper, Yamuna Middle, Banas, and Kali Sindh have negative minimum Sen slope values, implying that they are also experiencing a drought condition. Third, the sub-basins of Ram Ganga, Ghaghra, Chambal Lower, Gomti, Ghaghra Gomti Confluence, Tons, Son, Gandak, and Kosi have slightly negative to almost neutral minimum Sen's slope values, suggesting that they are experiencing a relatively mild drought condition or normal conditions. Finally, the sub-basin of Chambal Upper has a slightly positive minimum Sen's slope value, indicating that it is experiencing slightly more than average precipitation. Overall, the result indicates that many of the sub-basins are experiencing drought conditions based on the SPI_12 analysis of precipitation data. The severity of the drought varies, with some sub-basins experiencing more severe drought conditions than others. However, it is worth noting that the SPI_12 analysis only provides a snapshot of the current situation, and long-term trends should also be considered to fully understand the drought situation in these sub-basins.

Overall, the maximum Sen's slope values range from −0.000740 to 0.002645. Among the sub-basins with positive maximum Sen's slope values, Ram Ganga has the highest value of 0.002645, followed closely by Chambal Upper and Kali Sindh with values of 0.002507 and 0.002381, respectively. Yamuna Upper, Yamuna Middle, Banas, Ghaghra, Yamuna Lower, Chambal Lower, Gomti, and Ghaghra Gomti Confluence also have positive maximum Sen's slope values ranging from 0.002308 to 0.001017. On the other hand, six sub-basins have negative maximum Sen's slope values ranging from −0.000740 to −0.000123. Therefore, the sub-basins with positive maximum Sen's slope values are likely to have experienced more precipitation over the analyzed period, while the sub-basins with negative values experienced less precipitation.

Overall, the mean Sen's slope values range from a positive 0.001518 for the Chambal Upper sub-basin to a negative 0.002216 for the Bhagirathi sub-basin (Figure 5). First, the sub-basin with the highest mean Sen's slope value, Chambal Upper, stands out from the rest of the sub-basins with a positive value. This suggests that this sub-basin has received more precipitation than the other sub-basins during the period of analysis. Second, the sub-basins with the lowest mean Sen's slope values, Bhagirathi, Damodar, Kosi, Gandak, and Son, are all negative and have relatively large absolute values. This indicates that these sub-basins have received less precipitation than the other sub-basins during the period of analysis. Overall, the mean Sen's slope values of the SPI_12 analysis of precipitation data for the 19 sub-basins show that some sub-basins have received more precipitation than others during the period of analysis. The sub-basins with the lowest mean Sen's slope values are cause for concern, as they have received significantly less precipitation than the other sub-basins. This could have implications for water availability, agriculture, and other aspects of life in those areas.

4.2. Gravity Recovery and Climate Experiments – Drought Severity Index

The GRACE-DSI provides worldwide continuous drought monitoring for the whole terrestrial hydrologic cycle (i.e., snow, SW, soil moisture, and groundwater).

4.2.1. Descriptive analysis of winter GRACE-DSI

Following G-DSI analysis for the winter session, we discovered that exceptional drought episodes only occurred four times throughout the study region at grids S-1, S-2, S-3, and S-4, while severe drought was the most common drought event (183 times). In addition, 103 and 146 instances of light and moderate drought, respectively, were recorded. In this study, we showed no extreme drought occurrences over the entire study area. In total, 428 events were classified as 'near-normal', which is the maximum number of events for a single condition. On the other hand, slightly wet, moderately wet, and severely wet circumstances were observed 206, 119, and 71 times, respectively. Furthermore, 69 events were recorded as 'extremely wet', while only 3 events were 'exceptionally wet' over the study region.

The analysis of data collected from 74 grids in the region indicates a widespread trend toward increasing drought severity during the winter season. Specifically, 63 of these grids exhibit a significant decreasing trend in winter GRACE_DSI values, which strongly suggests that drought conditions in the region have been worsening. In contrast, only three grids demonstrate a significant increasing trend, and two others show a non-significant increasing trend. While these grids represent a minority, their presence reinforces the notion that increasing drought severity is a pervasive phenomenon across the study region. In addition, six grids display a non-significant decreasing trend, which may imply either a lack of statistical significance or insufficiently strong evidence of a decreasing trend. The implications of this trend are significant and far-reaching, as it could have serious impacts on sectors such as agriculture and water resources, which depend on a consistent and reliable supply of water.

The results show that the minimum Sen's slope values range from −0.089828 to −0.175235 across.

The sub-basin with the lowest minimum Sen's slope value is Chambal Upper with a value of −0.089828, while the sub-basin with the highest minimum Sen's slope value is Yamuna Upper with a value of −0.175152. On average, the sub-basins have a minimum Sen's slope value of −0.164, which indicates a moderate to low level of groundwater storage. The sub-basins Yamuna Upper, Above Ram Ganga Confluence, and Ram Ganga have the lowest minimum Sen slope values, suggesting a high level of groundwater depletion (Figure 6). In contrast, the sub-basin Chambal Upper has the highest minimum Sen's slope value, indicating a relatively stable groundwater storage. The findings as a whole show the substantial spatial diversity in groundwater storage throughout the sub-basins. While the sub-basins in the southern and eastern regions of India, such as Chambal Upper, Kali Sindh, Tons, Son, and Damodar, have relatively stable groundwater storage, the sub-basins in the northwestern and central regions, such as Yamuna Upper, Above Ram Ganga Confluence, and Ram Ganga, are more susceptible to groundwater depletion (Figure 11(a)). These results point to the necessity of groundwater management techniques that are region-specific to ensure the sustainable use of this essential resource. The range of the maximum Sen's slope values is between −0.166212 and 0.088779. Overall, the findings imply that the majority of sub-basins have maximum Sen's slope values that are negative, indicating a tendency toward declining winter groundwater storage. The sub-basins Ram Ganga, Above Ram Ganga Confluence, and Kosi have the highest maximum negative values for Sen's slope. Only three sub-basins (the Yamuna Lower, Kali Sindh, and Chambal Upper), however, have maximum Sen's slope values that are positive, demonstrating an upward trend in winter groundwater storage. Ram Ganga, Above Ram Ganga Confluence, and Kosi are the sub-basins with the biggest absolute maximum Sen's slope values, showing the most dramatic decreasing trend in winter groundwater storage. This might be the result of several factors, like excessive groundwater extraction or modifications to the pattern of precipitation. Damodar, Bhagirathi, and Banas are three sub-basins having substantially lower absolute

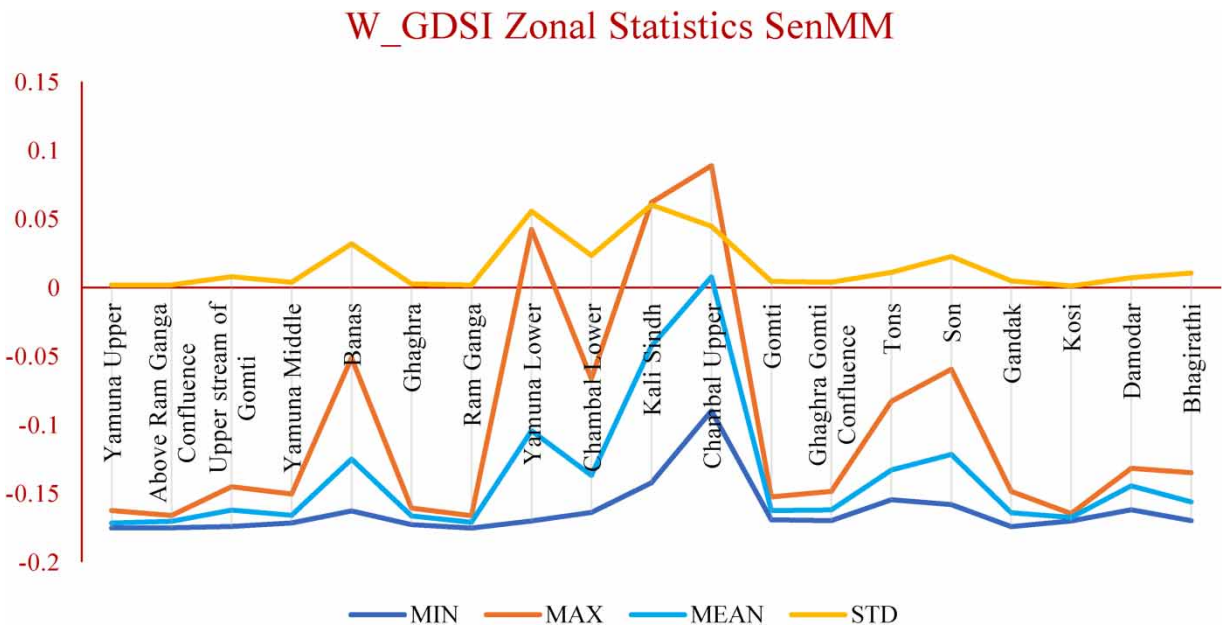

Figure 6 | Zonal statistical mean of winter GRACE-DSI in the Ganga basin.

maximum Sen's slope values. Overall, the findings imply that, with a few notable exceptions, the winter groundwater storage trend in the study area is primarily falling. The majority of the sub-basins have negative mean values, with the exception being Chambal Upper, which has a marginally positive mean value. The range of the mean values is from −0.171569 to 0.007773. The sub-basin with the lowest mean value is Yamuna Lower, which has a value of −0.104319, and the lowest negative mean value is in Kali Sindh, which is at −0.042698. Chambal Upper is the sub-basin with the highest negative mean value of −0.171569. The implication of the negative mean values is a decline in the sub-basin's overall winter water storage. Higher negative mean values may indicate more severe water scarcity, whereas lower negative mean values may indicate relative improvement in certain sub-basins. The water storage dynamics may alter throughout other seasons; therefore, it is important to keep in mind that the mean values only give an overview of the winter season. The amount of water stored in the sub-basins can also be impacted by additional factors, including climate change and human activity.

4.2.2. Descriptive analysis of summer GRACE-DSI

According to S-GDSI (GRACE-Drought Severity Index) data, the research area's grids S-16, S-60, and S-65 only saw three instances of extreme drought, compared to 138 moderate drought occurrences overall. The frequency analysis shows that exceptional drought conditions were only reported at 37 sites once, while there were 71 occasions when slight drought conditions were present. In addition, 119 events are under severe drought conditions. Overall, most of the events that happened over the study region were near-normal (561). However, in this summer's GDSI, there was not a single case of exceptionally wet conditions. Moreover, slight and moderate wet conditions were observed 136 and 216 times, whereas there were 87 and 38 events of severe wet and extreme wet conditions, respectively. Out of the 74 grids, the majority (63) exhibit a noteworthy declining pattern in summer GRACE_DSI, which is supported by a Z-score less than −1.96. This finding implies that the region has undergone a significant escalation in drought severity during the summers. Conversely, only three grids demonstrate a significant upward trend in summer GRACE_DSI, indicating that there could be some relief from drought conditions in these specific areas. In addition, six grids reveal a non-significant decrease in trend, while two grid show a non-significant increase in trend. This outcome suggests that there is no substantial trend in drought severity in those locations during the summers. Considering the significant decreasing trend in Summer GRACE_DSI observed in most grids, it is likely that the region experiences more recurrent and severe droughts in the summers. This phenomenon corresponds with the anticipated consequences of climate change, which may amplify the frequency and severity of droughts in numerous areas. Contrarily, the rising trend seen in a small number of grids may be attributable to regional variables, such as improved water management strategies or changes in land use, which may have reduced the intensity of the drought in those locations. Most of the grids show a large declining trend in summer GRACE_DSI, which is consistent with the effects of climate change, and the data show that the region has suffered a considerable increase in drought severity throughout the summers. This demonstrates the need for adequate action to reduce the negative consequences that droughts have on the affected communities.

The main finding of the analyses is that all the sub-basins have negative minimum Sen's slope values (Figure 7). This suggests a decline in the amount of terrestrial water stored in all the sub-basins over the summer. The Ram Ganga sub-basin has the lowest minimum Sen's slope value (−0.175235) which indicates that it has the greatest reduction in TWS when compared to all other sub-basins. The Chambal Upper sub-basin, on the other hand, has the greatest minimum Sen's slope value, at −0.089828, which denotes a somewhat slower decline in TWS over the summer. Another finding from the table is that the sub-basins with the highest minimum Sen's slope values are usually found in India's north, while those with the lowest values are found in the country's center and south.

This could be due to differences in rainfall patterns and water management practices in these regions. Overall, the result provides useful information on the seasonal changes in TWS in different sub-basins in India.

The result presents zonal statistics of the maximum Sen's slope values of summer GRACE DSI analysis of GRACE data of 19 sub-basins (Figure 7). The maximum values range from −0.166212 to 0.088779, indicating significant variation in the water storage trends across the sub-basins. The highest maximum value of 0.088779 is recorded in Chambal Upper, suggesting an increase in water storage during the summer. In contrast, the lowest maximum value of −0.166212 is observed in Ram Ganga, indicating a significant decrease in water storage during the summer. Most sub-basins, including Yamuna Upper, Above Ram Ganga Confluence, Yamuna Middle, Ghaghra, Gomti, Ghaghra Gomti Confluence, Kosi, and Bhagirathi, have negative maximum values, indicating decreasing water storage trends during the summer. However, the maximum values for the Yamuna Lower, Kali Sindh, and Damodar sub-basins are positive, indicating a rise in water storage over the summer. The highest

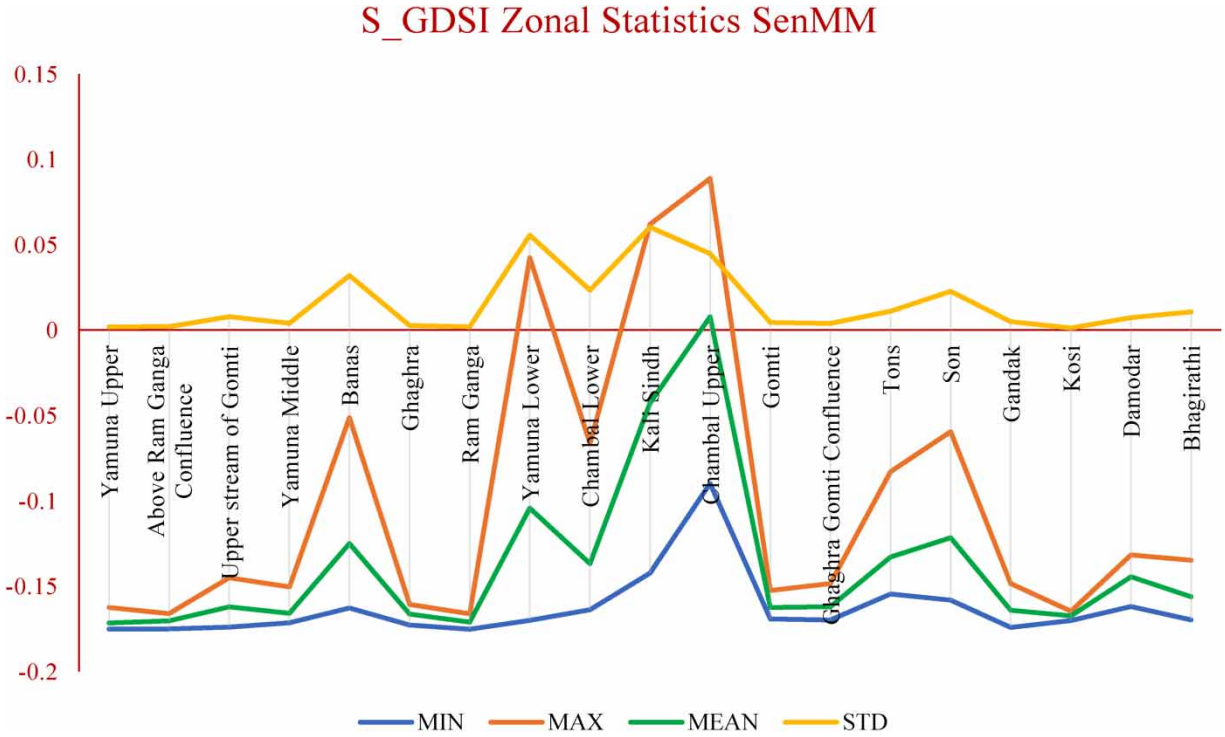

Figure 7 | Zonal statistical mean of summer GRACE-DSI in the Ganga basin.

values for the remaining sub-basins (Banas, Chambal Lower, Tons, Son, and Gandak) are close to zero, indicating that summertime water storage changes are unlikely to be significant. The zonal statistics of the maximum Sen's slope values, in general, show a considerable variation in water storage patterns throughout the sub-basins. The majority of sub-basins negative maximum values indicate a drop in water storage over the summer, which could be explained by higher evapotranspiration, lower precipitation, or anthropogenic activity. However, the positive maximum values in a few sub-basins (between −0.171569 and 0.007773) point to a rise in water storage, which may be caused by more precipitation or a decline in human activity. The table's primary features are its negative mean values; only one of the sub-basins has a somewhat positive number. The mean value for Yamuna Upper is −0.171569, while the mean value for Kali Sindh is −0.042698. In the majority of the sub-basins, the summertime TWS decreases, as indicated by the negative mean values. The only sub-basin with a marginally positive result is Kali Sindh, which would point to a marginal rise in TWS throughout the summer. Overall, the results show how seasonal variability affects TWS in various sub-basins. In addition, it highlights how crucial it is to manage and monitor water supplies to ensure their sustainable use in light of shifting climatic conditions.

4.2.3. Descriptive analysis of monsoon GRACE-DSI

As per the M-GDSI result, the frequency of extreme and exceptional drought conditions is the same as the S-GDSI data, but the occurrence of low, moderate, and severe drought is slightly different. By contrast, in this case, only one case of exceptional wet conditions happened at grid S-8. Overall, the rest of the wet conditions were observed almost exactly the same as S-GDSI.

In this case, the majority of the grid (66 out of 74) has shown a significant decreasing trend in Monsoon GRACE_DSI, indicating a reduction in surface SM over time. This trend has significant implications for agriculture, water resources, and the environment. Conversely, only five grids show a non-significant decreasing trend, while three grids show a non-significant increasing trend, implying insufficient evidence to determine the trend of surface SM in these areas. Meanwhile, none of the grids indicate a SIT in monsoon GRACE_DSI, highlighting a high level of consistency in the decreasing trend of surface SM across the study region. The downward trend in monsoon GRACE_DSI is concerning since it can lead to environmental and social challenges such as water scarcity, soil erosion, and reduced agricultural productivity. The trend's possible causes include climate change, deforestation, land-use change, and groundwater extraction. In addition, the decreasing trend in

monsoon GRACE_DSI aligns with the general trend of decreasing monsoon rainfall in the area over the past few decades. This trend is attributed to various factors, such as global warming, land-use change, and aerosol pollution. Furthermore, the study region is susceptible to natural disasters such as floods, droughts, and landslides, and the decreasing trend in monsoon GRACE_DSI could exacerbate the frequency and intensity of these disasters, leading to significant economic and social losses.

The main features of the data can be highlighted as follows (Figure 8):

- The minimum Sen's slope values for all sub-basins fall between −0.166554 and −0.109959, indicating a relatively narrow range of values.
- Chambal Upper has the lowest Sen's slope value of −0.109959, while Yamuna Upper has the highest value of −0.166554.
- The majority of sub-basins (13 out of 19) have a minimum Sen's slope value ranging from −0.160165 to −0.14161, suggesting that these sub-basins may have similar patterns of TWSA during monsoon season.
- Chambal Lower has a minimum Sen's slope value of −0.153496, which is slightly higher than the majority of sub-basins but still falls within the range of −0.160165 to −0.14161.
- Kali Sindh has the lowest Sen's slope value among the sub-basins within the range of −0.160165 to −0.14161, indicating a possible water scarcity issue in this sub-basin.
- Chambal Upper has a significantly lower Sen's slope value compared to all other sub-basins, indicating a higher degree of water scarcity in this region.

Overall, the information points to a rather restricted range of values for the minimum Sen's slope values for the 19 sub-basins. There are differences in the values as Chambal Upper has the lowest value and Yamuna Upper has the highest. During the monsoon season, most of the sub-basins exhibit a similar pattern of water availability, with 13 of 19 falling within a constrained range of −0.160165 to −0.14161. The lowest rating among these is for Kali Sindh, suggesting a potential

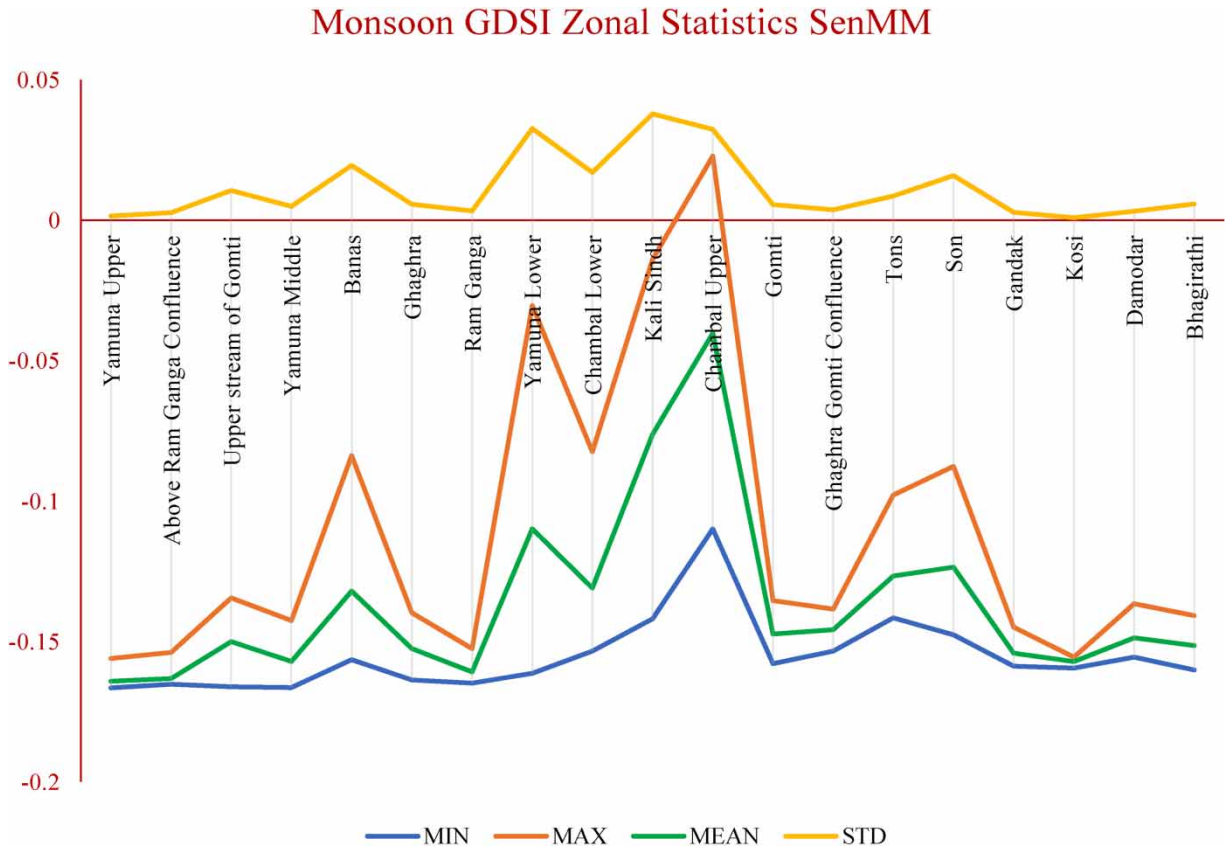

Figure 8 | Zonal statistical mean of monsoon GRACE-DSI in the Ganga basin.

problem with water availability. Chambal Lower is still within this range despite having a slightly higher value. The information demonstrates the necessity of further investigation and management of water resources in sub-basins with lower Sen's slope values, particularly in Chambal Upper and Kali Sindh.

The negative values of the maximum Sen's slope values, which show a declining trend in groundwater storage in most of the sub-basins, are the major highlights of the table (Table 4). The Kosi, Yamuna Upper, and Above Ram Ganga Confluence sub-basins exhibited the largest negative Sen's slope values. The upper, middle, and lower sub-basins of the Yamuna River basin were found to have negative maximum Sen's slope values. In addition, the maximum Sen's slope values in the Ganges River's Ram Ganga and Ghaghra sub-basins are negative. Contrarily, the maximum Sen's slope value for the Chambal Upper sub-basin is positive, indicating a rising trend in groundwater storage. A negative maximum Sen's slope value was found in the Kali Sindh sub-basin, which only suggests a modest decline in groundwater storage. Similar results may be seen for the Bhagirathi sub-basin, which shows a modest drop in groundwater storage and a moderate maximum negative Sen's slope value. The bulk of the sub-basins appear to be seeing a downward trend in groundwater storage, which could have a significant impact on the region's future water availability. To ensure the sustainability of water resources in the impacted regions, appropriate groundwater management measures are required, as shown by the negative values of maximum Sen's slope values. Yamuna Upper has the lowest mean value and Chambal Upper has the greatest mean value, with values ranging from −0.164192 to −0.040302. It generally seems that the majority of the sub-basins have negative mean values, which suggests that during the monsoon season, TWS decreases. Yamuna Upper, Yamuna Lower, and Kali Sindh have the lowest mean values, which may indicate that these regions experience more severe water stress during the monsoon season. Contrarily, the sub-basins with higher mean values, such as the Ganges and the Upper Chambal, would suggest that these regions have more consistent water supplies during the monsoon. The availability of water in these sub-basins may also be impacted by other factors such as rainfall, groundwater recharge, and irrigation methods. It is crucial to keep in mind that the figures indicate the mean of Sen's slope values.

4.2.4. Descriptive statistics of post-monsoon GRACE-DSI

The post-monsoon (PM)-GDSI recorded 67 (slight drought), 139 (moderate drought), and 122 (severe drought) cases, as well as 37 exceptional drought events, which is nearly identical to the S-GDSI and M-GDSI. In addition, a total of 561 cases of near-normal conditions occurred, with 84 events of severe wetness and 37 events of extreme wetness.

The data collected from 74 grids suggests a consistent decline in groundwater storage in the study region during the post-monsoon season over the years. Specifically, 66 out of 74 grids show a significant decreasing trend in post-monsoon GRACE_DSI, indicating the severity of the issue. This consistent decline could be attributed to several factors, such as over-exploitation of groundwater resources, climate change, and variability in rainfall patterns. In contrast, only one grid point out of the 74 shows a SIT in post-monsoon GRACE_DSI, implying an improvement in groundwater storage at that location. However, it is challenging to draw a conclusion based on this single grid, as it could be due to specific interventions or natural factors. In addition, four grids show an NSIT in post-monsoon GRACE_DSI, indicating an increasing trend that is not significant enough to reject the null hypothesis of no trend. Similarly, three grids show an NSDT in post-monsoon GRACE_DSI. The significant decreasing trend in post-monsoon GRACE_DSI across the majority of the grid highlights the potential stress and over-exploitation of groundwater resources.

The minimum Sen's slope values range from −0.102516 in the Chambal Upper sub-basin to −0.178548 in the Ghaghra sub-basin (Figure 9). Overall, the result depicts that the sub-basins with higher minimum Sen's slope values (such as Ghaghra, Yamuna Upper, and Above Ram Ganga Confluence) may have experienced more severe water stress during the post-

Table 4 | Band statistics of GRACE-DSI

Build parameter	W-GDSI	S-GDSI	M-GDSI	PM-GDSI	AN-GDSI
Minimum value	−0.18	−0.18	−0.17	−0.19	−0.18
Maximum value	0.09	0.09	0.02	0.06	0.09
Mean value	−0.13	−0.13	−0.13	0.14	−0.15
Standard deviation	0.05	0.05	0.03	0.04	0.05

GDSI, GRACE-Drought Severity Index; PM, post-monsoon.

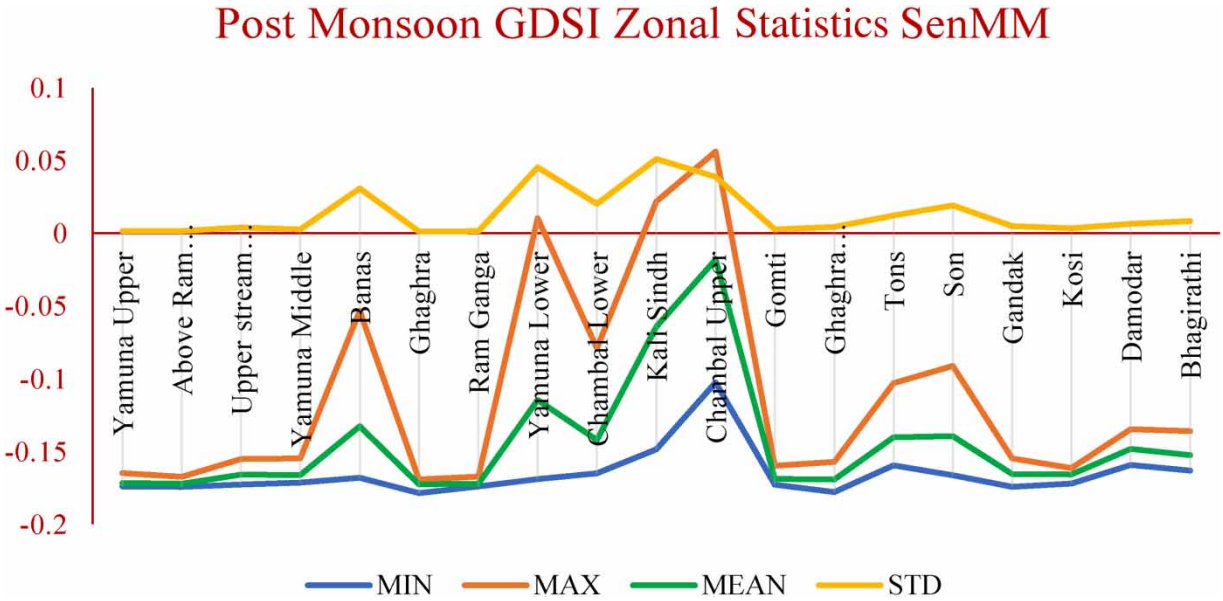

Figure 9 | Zonal statistical mean of post-monsoon GRACE-DSI in the Ganga basin.

monsoon period compared to sub-basins with lower minimum Sen's slope values (such as Chambal Upper and Kali Sindh). This may be due to factors such as low rainfall, high evapotranspiration, or excessive groundwater extraction. It could mean that the sub-basins with lower minimum Sen's slope values would have seen improved post-monsoon water availability. Hence, it is crucial to remember that the minimum Sen's slope values do not reflect long-term trends or the total water availability in the sub-basins; rather, they simply offer a snapshot of water availability within a given time period. To completely comprehend the state of the water resources in these sub-basins, additional research and monitoring are necessary.

The major highlight of the table is the negative maximum values of most of the sub-basins, which show a downward trend in groundwater storage (Figure 9). Ghaghra is the sub-basin with the highest negative value, indicating the greatest loss in groundwater storage. However, the highest values for the Yamuna Lower, Kali Sindh, Chambal Upper, and Gandak sub-basins are positive, showing a rising trend in groundwater storage. The increase in storage is less significant than the decrease in other sub-basins, though. With a minimum negative score of −0.053354, Banas is the sub-basin that has experienced the least loss in groundwater storage. Damodar and Bhagirathi are two additional sub-basins with comparatively modest negative values. The table summarizes a downward trend in groundwater storage for the majority of the sub-basins. It emphasizes the need for improved water management techniques and conservation measures to enable long-term sustainable groundwater use. Furthermore, the sub-basins with a growing trend in groundwater storage may offer insightful information into successful water management techniques that can be applied to other sub-basins to ensure a sustainable water supply. Based on the water balance, the mean Sen's slope values describe the temporal variations in the water storage in the sub-basins and can be either positive or negative. The negative figures in the table show that water storage decreased after the monsoon.

The main features of the table are as follows (Figure 9):

- The mean Sen's slope values of the sub-basins range from −0.172504 to −0.018045, with a mean of −0.142662.
- The sub-basin with the highest mean Sen's slope value is Chambal Upper, indicating an increase in water storage during the post-monsoon period.
- The sub-basin with the lowest mean Sen's slope value is Ghagra, indicating a significant decrease in water storage during the post-monsoon period.
- Most of the sub-basins have negative mean Sen's slope values, indicating a decrease in water storage during the post-monsoon period.

Overall, the table indicates that the post-monsoon period has led to a decrease in water storage in most of the sub-basins, with only Chambal Upper showing an increase. The significant decrease in Yamuna Lower and the negative mean Sen's

slope values of other sub-basins suggest the need for water management strategies to ensure sustainable water use in these regions.

4.2.5. Descriptive statistics of annual GRACE-DSI

Finally, an annual frequency analysis of the chosen study area showed 37 events of exceptional drought and only 3 events of extreme drought conditions on the same grid as S-GDSI. The most frequent drought conditions occurred in moderate drought conditions (140), while 121 events of severe drought were observed. According to the analysis, no exceptional wet conditions occurred during the period, with 86 events of severe wet and 39 extreme wet conditions observed.

The study analyzed 74 grids and found that 64 grids (86.5%) have experienced a significant decrease in annual GRACE_DSI, indicating a decline in groundwater storage in these regions over the study period. Meanwhile, only one grid (1.4%) showed a SIT in Annual GRACE_DSI, suggesting an increase in groundwater storage. Nevertheless, this increase was not significant enough to be considered a positive trend, and further analysis is required to understand its causes. In addition, three grids (4%) have shown a NSIT, implying a slight increase in groundwater storage that is not statistically significant. The groundwater storage in six grids (8%) has also shown an NSDT, which is also not statistically significant. There are a number of reasons why the majority of the grid has a substantial decreasing trend (SDT) in groundwater storage, including overuse of groundwater resources, a decline in rainfall, and an increase in water demand brought on by population expansion and economic development. Groundwater storage is on the decline, which could have negative effects on the ecosystem such as land subsidence and seawater intrusion. These results highlight how crucial it is to manage groundwater resources sustainably in the research area. Promotion of effective irrigation techniques, regulation of groundwater abstraction, rainwater collection, and preservation of wetlands and other natural recharge zones are some of the potential actions that might be taken to manage groundwater resources sustainably in the research area. Such actions can be taken to minimize the groundwater storage trend toward decline and guarantee the long-term viability of the local water supplies. In the majority of the sub-basins, the minimum Sen's slope values, which range from −0.110014 to −0.178903 (Figure 10), show a falling trend in water storage. This indicates that there is less water available in these sub-basins now than there was previously. Sen's slope values are lowest in Chambal Upper (−0.110014), Kali Sindh (−0.155462), and Son (−0.158854), showing a more dramatic falling trend in water storage than is the case in other sub-basins. Banas (−0.16888), Tons (−0.162691), and Damodar (−0.164626) had the highest Sen's slope values, indicating less in water storage than other sub-basins. Sen's slope values for the three sub-basins of the Yamuna River basin, Yamuna Upper, Yamuna Middle, and Yamuna Lower, range from −0.17496 to −0.178903,

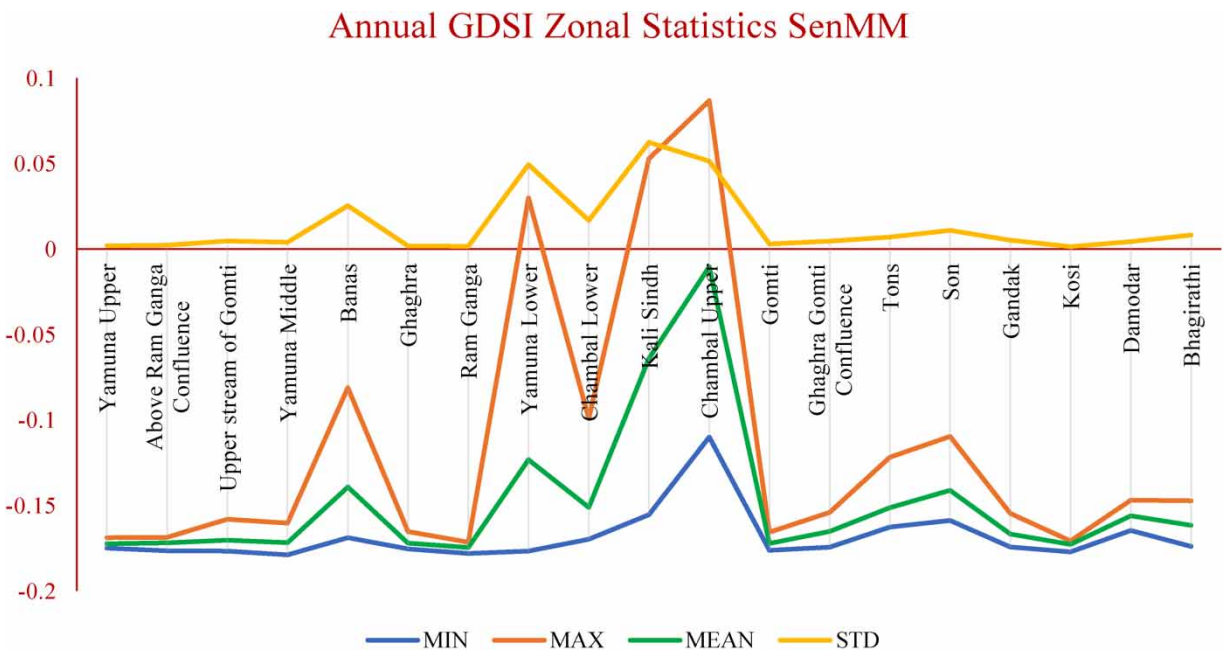

Figure 10 | Zonal statistical mean of annual GRACE-DSI in the Ganga basin.

suggesting a considerable decline in water storage in this basin. Compared to the Ghaghra sub-basin (−0.175471) and the Gomti sub-basin (−0.176259), the Sen's slope value for the Ghaghra Gomti Confluence sub-basin is comparatively lower (−0.174398). This shows a less severe water storage trend in the Ghaghra Gomti Confluence sub-basin compared to the other two sub-basins. The sub-basins maximum Sen's slope values range from −0.171514 to 0.086715. Ram Ganga and Chambal Upper have the highest maximum Sen's slope values, while Yamuna Lower and Kali Sindh have the lowest maximum Sen's slope values. Negative maximum Sen's slope values for any sub-basin suggest a downward trend of groundwater level during the study period, indicating that the drought conditions in certain areas are getting worse. Chambal Upper is the sub-basin with the highest positive maximum Sen's slope value, indicating that the area's groundwater levels are rising. Sub-basins with moderately negative maximum Sen's slope values, like Tons and Son, suggest a progressive fall in groundwater levels, which, if not reversed, could result in future drought conditions. The findings also show that the maximum Sen's slope values in some of the sub-basins, such as Kali Sindh and Yamuna Lower, are extremely low. This suggests that the groundwater levels in those places have remained comparatively steady during the course of the study, which is encouraging for the security of the water supply in those areas. According to Figure 10, the sub-basins mean Sen's slope values range from −0.172417 for Yamuna Upper to −0.010466 for Chambal Upper. The sub-basins Kali Sindh, Yamuna Lower, and Banas have the lowest mean Sen's slope values, indicating a less severe level of drought. On the other side, sub-basins including Ram Ganga, Yamuna Middle, and Ghaghra Gomti Confluence that have higher mean Sen's slope values are going through more severe droughts. The findings also imply that the Yamuna River basin, which has sub-basins with high mean Sen's slope values, is currently facing the worst drought conditions. On the other hand, the lower mean Sen's slope values in the sub-basins of Chambal Upper and Kali Sindh indicate better drought conditions. The graphic representation of GRACE-DSI Sen's slope is shown by Figure 11. The GRACE-DSI Sen's slope of the zonal statistical mean of the sub-basin is shown by Figure 12. Figure 13 shows the frequency analysis of different GRACE-DSI.

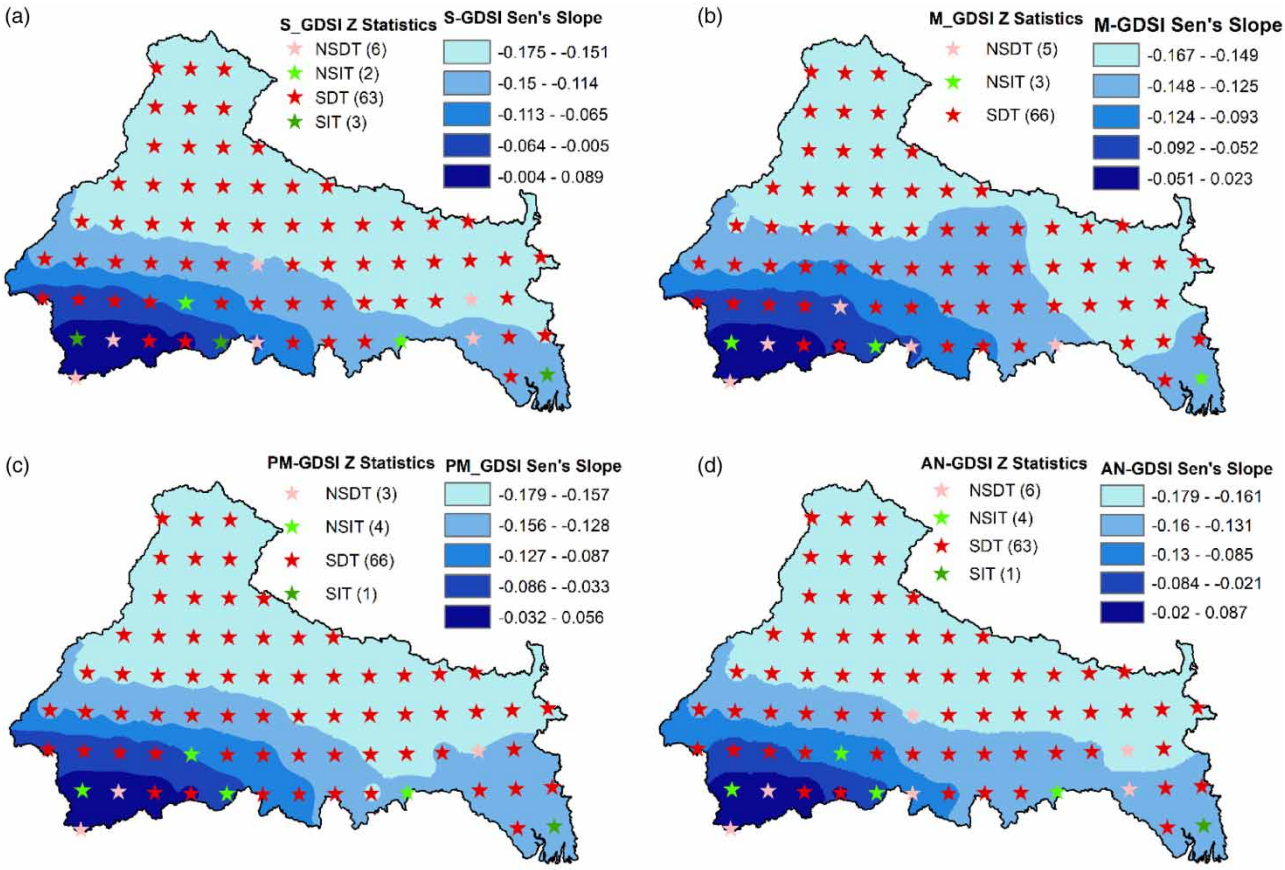

Figure 11 | Graphical representation of GRACE-DSI Sen's slope.

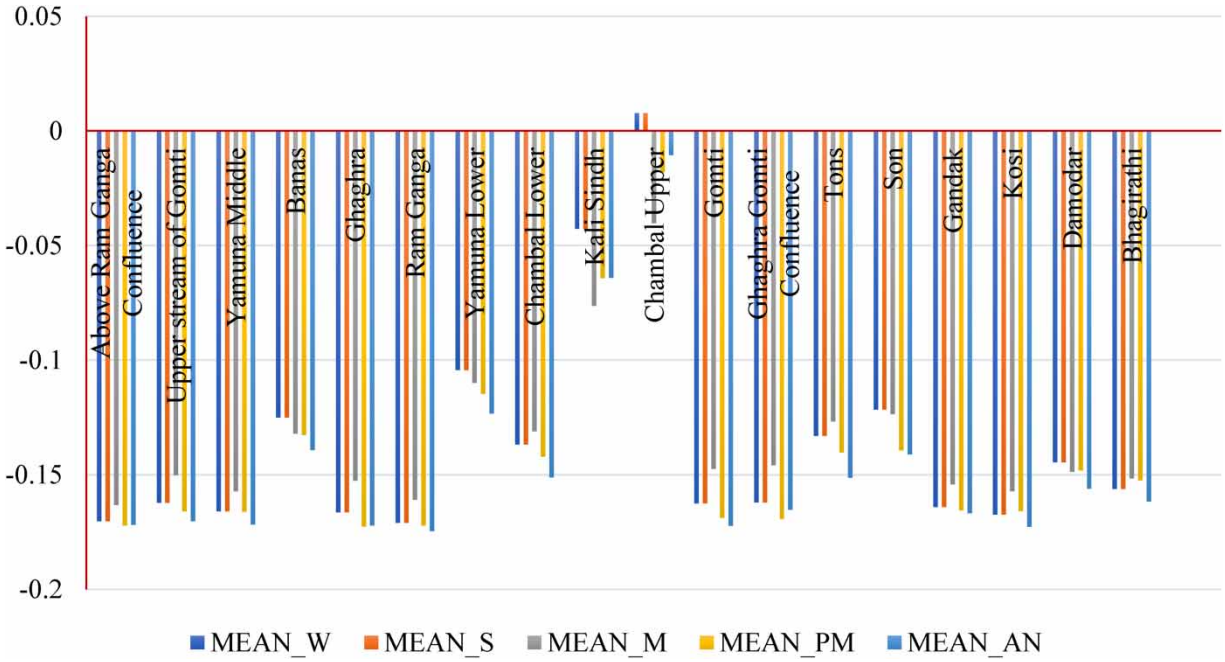

Figure 12 | GRACE-DSI Sen's slope of the zonal statistical mean of the sub-basin.

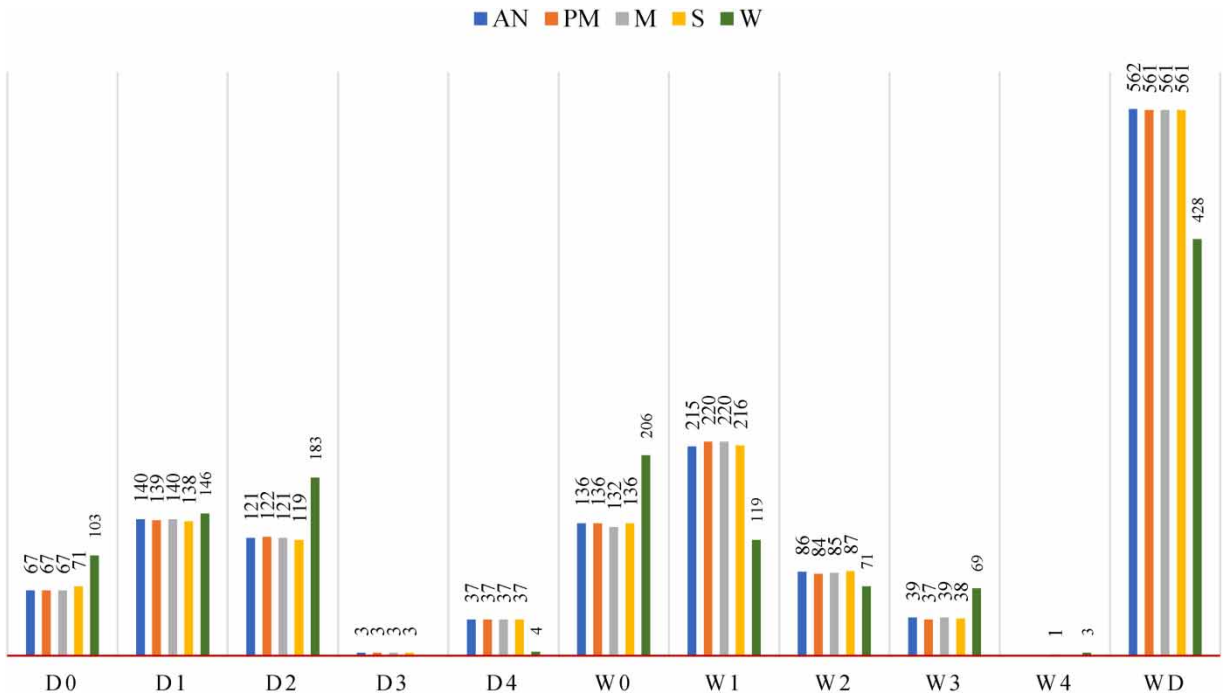

Figure 13 | Frequency analysis of different GRACE-DSI.

4.3. Vegetation-conditioned index (VCI)

The study examined 19 sub-basins to determine trends in VCI over a certain period. Results show that six sub-basins, comprising 31.6% of the total sub-basins, exhibited a significant increase in VCI with *Z*-significance values greater than 1.96. This finding implies a significant improvement in vegetation health in these sub-basins during the study period (Table 5).

Table 5 | Band statistics of VCI

Long period	VCI
Minimum value	14.38
Maximum value	92.47
Mean value	50.69
Standard deviation	7.71

On the other hand, 11 sub-basins, or 57.9% of the total sub-basins, exhibited a non-significant increase in VCI with *Z*-significance values ranging from 1.96 to zero. This suggests that while there has been a positive trend in vegetation health in these sub-basins, the trend is not statistically significant. Interestingly, none of the sub-basins showed a non-significant decrease in VCI over the study region, with *Z*-significance values ranging from zero to −1.96. However, two sub-basins, comprising 10.5% of the total sub-basins, showed a significant decrease in VCI with *Z*-significance values less than −1.96, implying a significant decline in vegetation health in these sub-basins during the study period.

5. DISCUSSION

In the 3-month SPI analysis, we observed that the Chambal Upper region (the South-western part of the Ganga River Basin) exhibited the wettest conditions (Figure 4(a)). This region, along with the Kali Sindh, Banas, and Yamuna Middle areas, experienced increased vegetation throughout the study period. The wetter conditions can be attributed to above-average precipitation in these areas, leading to higher water levels and greener landscapes. In contrast, the Above Ram Ganga Confluence, Bhagirtahi, and Damodar River basins faced the driest conditions. These regions experienced decreased water levels and reduced greenery during this period, likely due to below-average rainfall. In the 6-month SPI analysis, we found that the Chambal Upper region (the South-western part of the Ganga River Basin) continued to have the wettest conditions, along with the Yamuna Middle areas, Ram Ganga, and Ghaghra Gomti sub-basins (Figure 4(b)). These regions also experienced increased vegetation over the study period. Similar to the 3-month SPI analysis, the Above Ram Ganga Confluence, Bhagirtahi, and Damodar River basins faced relatively drier conditions compared to the wetter regions. These areas still had lower water levels and greener landscapes than the 3-month analysis, despite a modest rise in water levels. The mid-region of Ghanghra, Gomti, Ghaghra Gomti Confluence, and Yamuna Middle showed the wettest conditions in the 9-month SPI analysis (Figure 4(c)). Throughout the course of the study, these areas had an increase in vegetation, indicating positive moisture availability while the Gomti river basin's upper stream saw the driest weather. This area saw lower water levels and less greenery than other locations, presumably as a result of less precipitation. The eastern portion of the Ganga River Basin, where the Ghanghra, Gomti, Ghaghra, and Gomti Confluence is located, had the wettest conditions, according to the yearly SPI study (Figure 4(d)). Over the course of the study, the vegetation in these areas grew, indicating adequate rainfall. On the other hand, of all the sub-basins, the upper stream of the Gomti River basin saw the driest circumstances. Reduced vegetation and water levels in this area suggest below-average precipitation and likely water stress. Overall, the Ganga River Basin SPI analysis showed regional and temporal changes in precipitation and their impacts on water availability and vegetation development. In several sub-basins, wet conditions and increasing vegetation were seen, indicating good rainfall patterns. Other sub-basins, on the other hand, showed drier conditions, decreasing water levels, and diminished vegetation, indicating fewer precipitation amounts. Regional weather patterns, air circulation, geography, and climatic elements that affect the Ganga River Basin's rainfall patterns may all be contributing factors to these fluctuations.

The study's main result is that there is a general tendency in the area toward increased drought intensity annually, which strongly implies that the region's drought conditions have been getting worse. While a minority of grid points represent significant and non-significant increasing trend, and their presence reinforces the notion that increasing drought severity is a pervasive phenomenon across the study region. The study's findings are consistent with previous research on drought severity. The study by Vicente-serrano & Beguería (2014) analyzed the impact of temperature rise on drought severity worldwide and reported variable results. Another study by Aadhar & Mishra (2019) examined the effect of climate change on the frequency of drought over India and found that by the end of the 21st century, there was a 150% increase in the region experiencing severe drought. These studies have been based on drought indices obtained from low-resolution gridded climate data. According to the annual data, the region is experiencing droughts that are becoming more severe. Sectors that depend

on a steady and continuous supply of water, including agriculture and water resources, might be seriously impacted by this. The report also emphasizes the necessity for more study to comprehend this trend's sources and effects on society (Yu *et al.* 2018). This study has some drawbacks, including its single-region emphasis and dependance on information gathered from just 74 locations. To properly understand the reasons and effects of this trend, future research should broaden the study's geographic reach and gather data from more locations.

The study examined 19 sub-basins to discover any recurring patterns in the VCI throughout time. Results show that VCI has significantly increased in around one-third of all sub-basins (Figure 1). This finding implies that during the investigation, plant health in these sub-basins has greatly improved. On the other hand, almost half of the sub-basins total area saw a non-significant increase in VCI. Despite the fact that the vegetation health in these sub-basins has gotten better over time, the trend is not statistically significant. It is interesting to notice that there was no non-significant reduction in VCI across the research region's sub-basins. However, two sub-basins showed a significant reduction in VCI, indicating a significant decline in the health of the vegetation in these sub-basins over the course of the study (Figure 14). The findings show that during that time, vegetation health has typically increased throughout the research region. However, this improvement is not statistically significant for more than half of the total sub-basins investigated. The research also found that none of the sub-basins VCI declines in comparison to the study region were non-significant. This shows that the vegetation's health has not declined during the research period. These findings suggest that although the health of the vegetation has generally improved over the study period throughout the research area, this improvement is not statistically significant for more than half of the total sub-basins examined. The findings show that there are still certain areas where the vegetation's health has to be improved. This study has some limitations, including its single-region focus and reliance on remote sensing data rather than observations made on the ground. Future research into additional locations and the incorporation of ground-based observations with remote sensing data may advance this study.

To understand the environmental relationship of various drought indices, multi-point pixel-based correlation studies were carried out over the long period average mean. The degree of similarity between various parameters (GRACE-DSI [W, M, PM], SPI [3,6,9,12], and VCI) was determined by correlation analysis; a relationship between a parameter and a value on a scale of −1 to +1 indicates a negative relationship and a positive relationship, respectively (Hasan & Rai 2020). The correlation coefficient matrix of the teleconnection indices was evaluated on temperature and precipitation in Iran (Ahmadi *et al.* 2022).

The correlation matrix provided offers insights into the intricate relationships among various drought indices, including the GRACE-DSI for different seasons, SPI across different time frames, and VCI. The correlation values, ranging from −1 to 1,

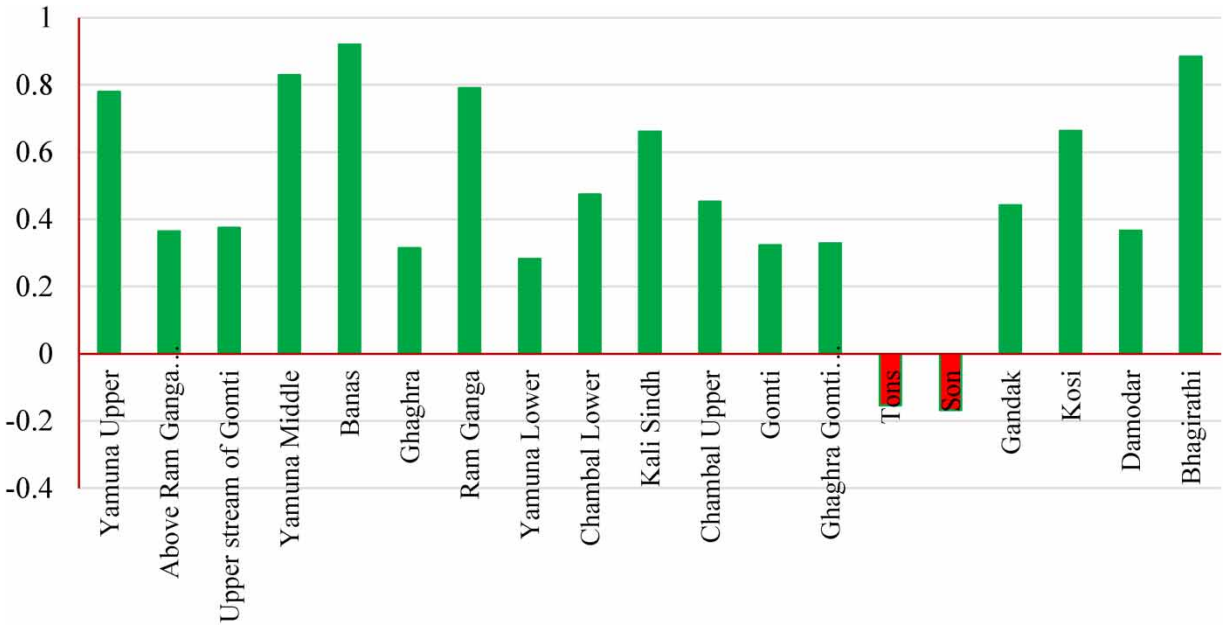

Figure 14 | VCI Sen's slope zonal statistical mean of sub-basin trend.

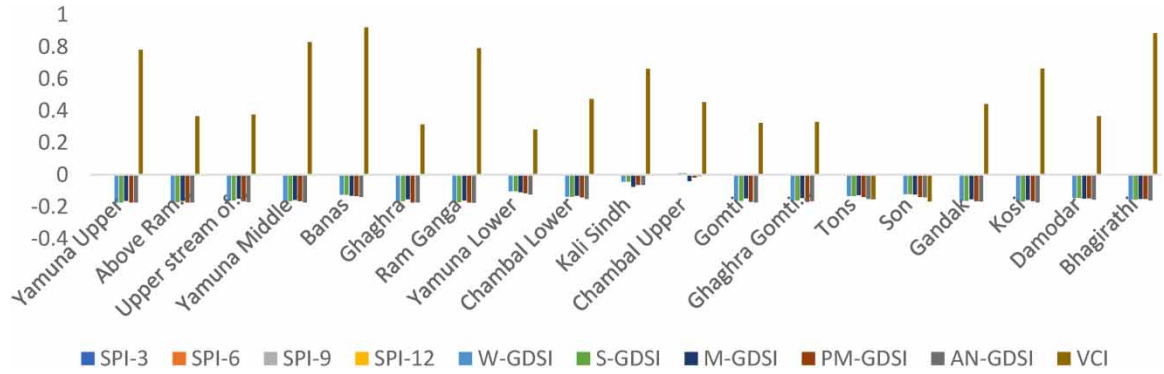

Figure 15 | Zonal statistical mean of future trend using Sen's slope.

provide a nuanced understanding of how these indices interact: where 1 denotes a perfect positive correlation, −1 is a perfect negative correlation, and 0 is a no connection.

There is the strongest positive correlation found between SPI-9 and SPI-12, 0.87469 indicates that when the dryness is high for 9 months, it is very likely to persist and be high for 12 months as well. Conversely, robust negative correlation surfaces between GRACE-DSI-PM (Drought Severity Index – Post Monsoon) and SPI-3, −0.70152 signifies a substantial opposing trend, suggesting that elevated post-monsoon drought severity tends to coincide with diminished precipitation levels in the preceding three months. For instance, it could indicate that high drought severity measured by one index during a specific period is likely followed by a significant improvement in drought conditions as measured by the other index. This information would be valuable for understanding and potentially predicting drought patterns.

Further examination of the correlation matrix unveils notable trends and patterns within the dataset. For instance, there is a moderate positive correlation between SPI-3 and SPI-6 (0.71078), GRACE-DSI_W and SPI-3 (0.50016), SPI-6 and SPI-9 (0.47756), as well as indicating consistency in precipitation patterns over successive periods. In addition, a moderate negative correlation exists between VCI and GRACE-DSI_W (−0.42131), suggesting that increased winter drought severity corresponds with decreased vegetation health.

6. CONCLUSION

After analyzing the precipitation, GRACE-DSI, and VCI multi-temporal datasets, we have concluded that the Ganga River Basin will experience an increasing trend of drought over the study period. Specifically, in the short-term (3-month SPI) analysis, the south-western region is projected to have more water availability, while other regions are facing scarcity of water. However, in the SPI-6 analysis, water availability in the south-western region has decreased while the northern and eastern regions are showing an increasing trend of water availability. The 9-month SPI results indicate that the eastern part of the Ganga River basin and a small part of the northern region have wet conditions, while the rest of the region experiences water scarcity throughout the basin. The zonal mean of all the sub-basins shows declining GRACE-DSI in all seasons except Upper Chambal, which shows a positive increase in winter and summer. All sub-basins show a positive increase in vegetation health dynamics except Sone and Tons sub-basins, which have decreased vegetation health. In conclusion, this study can aid in taking appropriate measures for future water security in the affected region. The findings of this study can be utilized by policymakers and water resource managers to implement effective drought mitigation strategies in the region (Figure 15). By understanding the spatial and temporal patterns of drought, the government can prioritize the allocation of resources toward areas that are most affected by drought, thereby reducing the impact of drought on agricultural productivity and livelihoods. This study also highlights the need for sustainable water resource management practices in the Ganga Basin, including the promotion of water harvesting and conservation techniques, to ensure long-term water security in the region to achieve agenda 2030 of the United Nations Sustainable Development Goals.

ACKNOWLEDGEMENTS

The authors would like to acknowledge the support provided by the Researchers Supporting Project Number RSP2024R297, King Saud University, Riyadh, Saudi Arabia.

DATA AVAILABILITY STATEMENT

All relevant data are included in the paper or its Supplementary Information.

CONFLICT OF INTEREST

The authors declare there is no conflict.

REFERENCES

Aadhar, S. & Mishra, V. 2019 *Impact of Climate Change on Drought Frequency Over India*.

Ahmad, T., Pandey, A. C. & Kumar, A. 2022 Long-term precipitation monitoring and its linkage with flood scenario in changing climate conditions in Kashmir valley. *Geocarto International* **37** (19), 5497–5522. https://doi.org/10.1080/10106049.2021.1923829.

Ahmadi, F., Tahroudi, M. N., Mirabbasi, R., Khalili, K. & Jhajharia, D. 2018 Spatiotemporal trend and abrupt change analysis of temperature in Iran. **321**, 314–321. https://doi.org/10.1002/met.1694.

Ahmadi, M., Kamangar, M., Salimi, S., Hosseini, S. A., Khamoushian, Y., Heidari, S., Moghim, G. M., Saeidi, V., Bakhshi, I. & Yarmoradi, Z. 2022 A new approach in evaluation impacts of teleconnection indices on temperature and precipitation in Iran. *Theoretical and Applied Climatology* **150** (1), 15–33.

Akhtar, S. 2023 Spatial-temporal trends mapping and geostatistical modelling of groundwater level depth over northern parts of Indo-Gangetic Basin, India. *Journal of Geography, Environment and Earth Science International* **27** (10), 96–112.

Akhtar, S. & Rampurawala, A. 2024 Integrating remote sensing data and MODFLOW modeling for sustainable groundwater resource management and monitoring in the Guinea Region, West Africa. *Journal of Geography, Environment and Earth Science International* **28** (1), 50–64.

Aksel, M. 2021 *Drought Analysis for the Seyhan Basin with NDVI and VCI Vegetation Indices*.

Aldrees, A., Hasan, M. S. U., Rai, A. K., Akhtar, M. N., Khan, M. A., Saif, M. M., Ahmad, N. & Islam, S. 2023 On the precipitation trends in global major metropolitan cities under extreme climatic conditions: An analysis of shifting patterns. *Water* **15** (3), 383. https://doi.org/10.3390/w15030383.

Alharbi, R. S., Nath, S., Faizan, O. M., Hasan, M. S. U., Alam, S., Khan, M. A., Bakshi, S., Sahana, M. & Saif, M. M. 2022 Assessment of drought vulnerability through an integrated approach using AHP and geoinformatics in the Kangsabati River Basin. *Journal of King Saud University-Science* **34** (8), 102332. https://doi.org/10.1016/j.jksus.2022.102332.

Boqer, S. & Science, O. 2009 Use of NDVI and land surface temperature for drought assessment: Merits and limitations. 618–633. https://doi.org/10.1175/2009JCLI2900.1.

Cheng, M. & Tapley, B. D. 2004 Variations in the Earth's oblateness during the past 28 years. *Journal of Geophysical Research: Solid Earth* **109**. https://doi.org/10.1029/2004JB003028.

Cheval, S. 2016 *The Standardized Precipitation Index – an Overview*.

Dangar, S. & Mishra, V. 2021 Natural and anthropogenic drivers of the lost groundwater from the Ganga River basin. *Environmental Research Letters* **16** (11), 114009. https://doi.org/10.1088/1748-9326/ac2ceb.

Das, J., Gayen, A., Saha, P. & Kumar, S. 2020 Meteorological drought analysis using standardized precipitation index over Luni River Basin in Rajasthan, India. *SN Applied Sciences* **2** (9), 1–17. https://doi.org/10.1007/s42452-020-03321-w.

Gerdener, H., Engels, O. & Kusche, J. 2020 A framework for deriving drought indicators from the Gravity Recovery and Climate Experiment (GRACE). *Hydrology and Earth System Sciences* **24** (1), 227–248. https://doi.org/10.5194/hess-24-227-2020.

Gocic, M. & Trajkovic, S. 2013 Analysis of changes in meteorological variables using Mann–Kendall and Sen's slope estimator statistical tests in Serbia. *Global and Planetary Change* **100**, 172–182. https://doi.org/10.1016/j.gloplacha.2012.10.014.

Hadri, A., Saidi, M. E. M. & Boudhar, A. 2021 Multiscale drought monitoring and comparison using remote sensing in a Mediterranean arid region: A case study from west-central Morocco. *Arabian Journal of Geosciences* **14**, 1–18.

Hamed, K. H. & Rao, A. R. 1998 A modified Mann–Kendall trend test for autocorrelated data. *Journal of Hydrology* **204** (1–4), 182–196.

Hasan, M. S. U. & Rai, A. K. 2020 Groundwater quality assessment in the lower Ganga Basin using entropy information theory and GIS. *Journal of Cleaner Production* **274**, 123077.

Hasan, M. S. U. & Rai, A. K. 2023 Suitability of the lower Ganga basin groundwater for irrigation, using hydrogeochemical parameters and land-use dynamics. *Environmental Science and Pollution Research* **30** (55), 116831–116847.

Hasan, M. S. U., Rai, A. K., Ahmad, Z., Alfaisal, F. M., Khan, M. A., Alam, S. & Sahana, M. 2022 Hydrometeorological consequences on the water balance in the Ganga river system under changing climatic conditions using land surface model. *Journal of King Saud University-Science* **34** (5), 102065.

Hasan, M. S. U., Saif, M. M., Ahmad, N., Rai, A. K., Khan, M. A., Aldrees, A., Khan, W. A., Mohammed, M. K. A. & Yaseen, Z. M. 2023 Spatiotemporal analysis of future trends in terrestrial water storage anomalies at different climatic zones of India UsingGRACE/GRACE-FO. *Sustainability* **15** (2), 1572. https://doi.org/10.3390/su15021572.

Hasan, M. S. U., Rai, A. K., Fatma, A., Nawaz, N., Aldrees, A., Khan, M. A. & Majdi, A. 2024 Assessment of future trends and spatial orientation of groundwater resources as an essential climate variable in the Ganga Basin. *Groundwater for Sustainable Development* **26**. https://doi.org/10.1016/j.gsd.2024.101201.

Hassan, S., Masood, M. U., Haider, S., Anjum, M. N., Hussain, F., Ding, Y., Shangguan, D., Rashid, M. & Nadeem, M. U. 2023 Investigating the effects of climate and land use changes on Rawal dam reservoir operations and hydrological behavior. *Water* **15**, 12. https://doi.org/10.3390/w15122246.

Jacob, T., Wahr, J., Pfeffer, W. T. & Swenson, S. 2012 Recent contributions of glaciers and ice caps to sea level rise. *Nature* **482**, 514–518. https://doi.org/10.1038/nature10847.

Jain, C. K. & Singh, S. 2020 Impact of climate change on the hydrological dynamics of River Ganga, India. https://doi.org/10.2166/wcc.2018.029.

Jena, S., Kumar, R., Ramadas, M., Mohanty, B. P., Kumar, A. & Kishore, S. 2021 Characterization of groundwater variability using hydrological, geological, and climatic factors in data-scarce tropical savanna region of India. *Journal of Hydrology: Regional Studies* **37**, 100887. https://doi.org/10.1016/j.ejrh.2021.100887.

Jos, L., Rangel, H. Á., Carlos, L. & Herazo, S. 2022 *Adjustment of the Standardized Precipitation Index (SPI) for the Evaluation of Drought in the Arroyo Pechel í n Basin, Colombia, Under Zero Monthly Precipitation Conditions*.

Kalura, P. 2021 Assessment of hydrological drought vulnerability using geospatial techniques in the Tons River Basin, India. *Journal of the Indian Society of Remote Sensing* **7**. https://doi.org/10.1007/s12524-021-01413-7.

Kamble, D. B., Gautam, S., Bisht, H., Rawat, S. & Kundu, A. 2021 Drought assessment for kharif rice using standardized precipitation index (SPI) and vegetation condition index (VCI). *Journal of Agrometeorology* **21** (2), 182–187. https://doi.org/10.54386/jam.v21i2.230.

Karam, S., Zango, B. S., Seidou, O., Perera, D., Nagabhatla, N. & Tshimanga, R. M. 2023 Impacts of climate change on hydrological regimes in the Congo River Basin. *Sustainability (Switzerland)* **15** (7). https://doi.org/10.3390/su15076066.

Khouni, I., Louhichi, G. & Ghrabi, A. 2021 Environmental Technology & Innovation Use of GIS based Inverse Distance Weighted interpolation to assess surface water quality: Case of Wadi El Bey, Tunisia. *Environmental Technology & Innovation* **24**, 101892. https://doi.org/10.1016/j.eti.2021.10189.

Kubicz, J. 2018 *The Application of Standardized Precipitation Index (SPI) to Monitor Drought in Surface and Groundwaters. 00082*.

Kumar, D. 2017 River Ganges-historical, cultural and socioeconomic attributes. *Aquatic Ecosystem Health and Management* **20** (1–2), 8–20. https://doi.org/10.1080/14634988.2017.1304129.

Landerer, F. W. & Swenson, S. C. 2012 Accuracy of scaled GRACE terrestrial water storage estimates. *Water Resource Research* **48**. https://doi.org/10.1029/2011WR011453.

Liu, H., Wu, J. & Xu, Y. 2019 Investigating the effects of precipitation on drought in the Hanjiang river basin using SPI. *Journal of Water and Climate Change* **10** (4), 977–992. https://doi.org/10.2166/wcc.2018.102.

Liu, X., Feng, X., Ciais, P., Fu, B., Hu, B. & Sun, Z. 2020 GRACE satellite-based drought index indicating increased impact of drought over major basins in China during 2002–2017. *Agricultural and Forest Meteorology* **291**. https://doi.org/10.1016/j.agrformet.2020.108057.

Lundberg, S. M. & Lee, S. 2017 *A Unified Approach to Interpreting Model Predictions. November*.

McKee, T. B., Doesken, N. J. & Kleist, J. 1993 The relationship of drought frequency and duration to time scales. In: *8th Conference on Applied Climatology, Anaheim*, 17-22 January 1993, 179–184.

Mehta, D. & Yadav, S. M. 2021 An analysis of rainfall variability and drought over Barmer District of Rajasthan, Northwest India. *Water Supply* **21** (5), 2505–2517. https://doi.org/10.2166/ws.2021.053.

Mehta, D. & Yadav, S. M. 2022 Temporal analysis of rainfall and drought characteristics over Jalore District of S-W Rajasthan. *Water Practice and Technology* **17** (1), 254–267. https://doi.org/10.2166/wpt.2021.114.

Mehta, D., Yadav, S., Ladavia, C. & Caloiero, T. 2023 Drought projection using GCM & statistical downscaling technique: A case study of Sirohi District. *Results in Engineering* **20**. https://doi.org/10.1016/j.rineng.2023.101605.

Meshram, S. G., Gautam, R. & Kahya, E. 2018 Drought analysis in the Tons River Basin, India during 1969–2008. 939–951. https://doi.org/10.1007/s00704-017-2129-2.

Mohammed, S., Alsafadi, K., Enaruvbe, G. O. & Bashir, B. 2022 Assessing the impacts of agricultural drought (SPI/SPEI) on maize and wheat yields across Hungary. *Scientific Reports* 1–19. https://doi.org/10.1038/s41598-022-12799-w.

Molla, S. H., Rukhsana & Hasan, M. S. U. 2023 Deployment of entropy information theory in the Indian Sundarban region using hydrogeochemical parameters and GIS for assessment of irrigation suitability. *Environmental Monitoring and Assessment* **195** (10), 1227. https://doi.org/10.1007/s10661-023-11847-w.

Moors, E. J., Groot, A., Biemans, H., Terwisscha, C., Scheltinga, V., Siderius, C., Stoffel, M., Huggel, C., Wiltshire, A., Mathison, C., Ridley, J., Jacob, D., Kumar, P., Bhadwal, S., Gosain, A. & Collins, D. N. 2011 Adaptation to changing water resources in the Ganges basin, northern India. **4**. https://doi.org/10.1016/j.envsci.2011.03.005.

Mukherjee, A. & Ramachandran, P. 2018 Prediction of GWL with the help of GRACE TWS for unevenly spaced time series data in India: Analysis of comparative performances of SVR, ANN and LRM. *Journal of Hydrology* **558**, 647–658. https://doi.org/10.1016/j.jhydrol.2018.02.005.

Pai, D. S., Rajeevan, M., Sreejith, O. P., Mukhopadhyay, B. & Satbha, N. S. 2014 Development of a new high spatial resolution (0.25 × 0.25) long period (1901–2010) daily gridded rainfall data set over India and its comparison with existing data sets over the region. *Mausam* **65** (1), 1–18.

Pandey, S. & Rao, A. D. 2019 Impact of approach angle of an impinging cyclone on generation of storm surges and its interaction with tides and wind waves. *Journal of Geophysical Research: Oceans* **124** (11), 7643–7660. https://doi.org/10.1029/2019JC015433.

Prasad, P., Loveson, V. J., Kotha, M. & Yadav, R. 2020 Application of machine learning techniques in groundwater potential mapping along the west coast of India. *GIScience & Remote Sensing* **00** (00), 1–18. https://doi.org/10.1080/15481603.2020.1794104.

Qian, X., Liang, L., Shen, Q. & Sun, Q. 2016 Drought trends based on the VCI and its correlation with climate factors in the agricultural areas of China from 1982 to 2010. *Environmental Monitoring and Assessment*. https://doi.org/10.1007/s10661-016-5657-9.

Qiu, J., Shen, Z. & Xie, H. 2023 Drought impacts on hydrology and water quality under climate change. *Science of the Total Environment* **858**. https://doi.org/10.1016/j.scitotenv.2022.159854.

Quiring, S. M. & Ganesh, S. 2010 Agricultural and forest meteorology evaluating the utility of the Vegetation Condition Index (VCI) for monitoring meteorological drought in Texas. **150**, 330–339. https://doi.org/10.1016/j.agrformet.2009.11.015.

Rawat, S., Ganapathy, A. & Agarwal, A. 2022 Drought characterization over Indian sub-continent using GRACE-based indices. *Scientific Reports* 1–15. https://doi.org/10.1038/s41598-022-18511-2.

Rehman, S., Hasan, M. S. U., Rai, A. K., Avtar, R. & Sajjad, H. 2021 Assessing flood-induced ecological vulnerability and risk using GIS-based in situ measurements in Bhagirathi sub-basin, India. *Arabian Journal of Geosciences* **14**, 1–17.

Rehman, S., Hasan, M. S. U., Rai, A. K., Rahaman, M. H., Avtar, R. & Sajjad, H. 2022 Integrated approach for spatial flood susceptibility assessment in Bhagirathi sub-basin, India using entropy information theory and geospatial technology. *Risk Analysis* **42** (12), 2765–2780.

Rezaiy, R. & Shabri, A. 2023 Drought forecasting using W-ARIMA model with standardized precipitation index. *Journal of Water and Climate Change* **14** (9), 3345–3367. https://doi.org/10.2166/wcc.2023.431.

Rodell, M., Houser, P. R., Jambor, U., Gottschalck, J., Mitchell, K., Meng, C.-J., Arsenault, K., Cosgrove, B., Radakovich, J., Bosilovich, M., Entin, J. K., Walker, J. P., Lohmann, D. & Toll, D. 2004 The global land data assimilation system. *Bulletin of the American Meteorological Society* **85** (3), 381–394. https://doi.org/10.1175/BAMS-85-3-381.

Satishkumar, K., Rathnam, E. V. & Sridhar, V. 2020 Tracking seasonal and monthly drought with GRACE-based terrestrial water storage assessments over major river basins in South India. *Science of the Total Environment* 142994. https://doi.org/10.1016/j.scitotenv.2020.142994.

Sazib, N., Mladenova, I. & Bolten, J. 2018 Leveraging the google earth engine for drought assessment using global soil moisture data. *Remote Sensing* **10** (8). https://doi.org/10.3390/rs10081265.

Shah, R., Bharadiya, N. & Manekar, V. 2015 Drought index computation using Standardized Precipitation Index (SPI) method for Surat District, Gujarat. *Aquatic Procedia* **4** (Icwrcoe), 1243–1249. https://doi.org/10.1016/j.aqpro.2015.02.162.

Siebert, S., Kummu, M., Porkka, M., Döll, P., Ramankutty, N. & Scanlon, B. R. 2015 A global data set of the extent of irrigated land from 1900 to 2005. *Hydrology and Earth System Sciences* **19** (3), 1521–1545.

Singh, A. K., Tripathi, J. N., Kotlia, B. S., Singh, K. K. & Kumar, A. 2018 Monitoring groundwater fluctuations over India during Indian Summer Monsoon (ISM) and Northeast monsoon using GRACE satellite data set: Impact on agriculture. *Quaternary International*. https://doi.org/10.1016/j.quaint.2018.10.036.

Sinha, D., Syed, T. H. & Reager, J. T. 2019 Utilizing combined deviations of precipitation and GRACE-based terrestrial water storage as a metric for drought characterization: A case study over major Indian river basins. *Journal of Hydrology* **572**, 294–307. https://doi.org/10.1016/j.jhydrol.2019.02.053.

Tefera, A. S. & Bello, J. O. A. N. J. 2019 Comparative analyses of SPI and SPEI as drought assessment tools in Tigray Region, Northern Ethiopia. *SN Applied Sciences* **1** (10), 1–14. https://doi.org/10.1007/s42452-019-1326-2.

Tirivarombo, S., Osupile, D. & Eliasson, P. 2018 Drought monitoring and analysis: Standardised Precipitation Evapotranspiration Index (SPEI) and Standardised Precipitation Index (SPI). *Physics and Chemistry of the Earth*. https://doi.org/10.1016/j.pce.2018.07.001.

Vermote, E. and NOAA CDR Program 2019 *NOAA Climate Data Record (CDR) of AVHRR Normalized Difference Vegetation Index (NDVI), Version 5*. NOAA National Centers for Environmental Information. https://doi.org/10.7289/V5ZG6QH9.

Vermote, E. and NOAA CDR Program 2022 *NOAA Climate Data Record (CDR) of VIIRS Normalized Difference Vegetation Index (NDVI), Version 1*. NOAA National Centers for Environmental Information. https://doi.org/10.25921/gakh-st76.

Vicente-serrano, S. M. & Beguería, S. 2014 Evidence of increasing drought severity caused by temperature rise in southern Europe. https://doi.org/10.1088/1748-9326/9/4/044001.

Vishwakarma, B. D. 2020 Monitoring droughts from GRACE. **8**, 1–6. https://doi.org/10.3389/fenvs.2020.584690.

Wiese, D. N., Landerer, F. W. & Watkins, M. M. 2016 Quantifying and reducing leakage errors in the JPL RL05M GRACE mascon solution. *Water Resources Research* **52**, 7490–7502. doi:10.1002/2016WR019344.

Yu, H., Zhang, Q., Sun, P. & Song, C. 2018 Impact of droughts on winter wheat yield in different growth stages during 2001–2016 in Eastern China. *International Journal of Disaster Risk Science* **9** (3), 376–391. https://doi.org/10.1007/s13753-018-0187-4.

Zhao, M., Velicogna, G. A.,I. & Kimball, J. S. 2017 A global gridded dataset of GRACE drought severity index for 2002–2014: Comparison with PDSI and SPEI and a case study of the Australia Millennium drought. *Journal of Hydrometeorology* **18**, 2117–2129. https://doi.org/10.1175/JHM-D-16-0182.1.

First received 17 January 2024; accepted in revised form 15 July 2024. Available online 26 July 2024